Functionally distinct PI 3-kinase pathways regulate myelination in the peripheral nervous system

Bradley A. Heller,[1] Monica Ghidinelli,[3] Jakob Voelkl,[4] Steven Einheber,[5] Ryan Smith,[1] Ethan Grund,[1] Grant Morahan,[6] David Chandler,[6] Luba Kalaydjieva,[6] Filippo Giancotti,[7] Rosalind H. King,[8] Aniko Naray Fejes-Toth,[9] Gerard Fejes-Toth,[9] Maria Laura Feltri,[3] Florian Lang,[4] and James L. Salzer[1,2]

[1]Neuroscience Institute and [2]Departments of Neuroscience and Physiology and Neurology, NYU Langone Medical Center, New York, NY 10016
[3]University of Buffalo School of Medicine, Hunter James Kelly Research Institute, Buffalo, NY 14214
[4]Department of Physiology, University of Tübingen, 72076 Tübingen, Germany
[5]Department of Medical Laboratory Sciences, Hunter College, City University of New York, New York, NY 10010
[6]Western Australian Institute for Medical Research/Centre for Medical Research, The University of Western Australia, Perth 6009, Australia
[7]Department of Cell Biology, Memorial Sloan-Kettering Cancer Center, New York, NY 10065
[8]UCL Institute of Neurology, University College London, London NW3 2PF, England, UK
[9]Department of Physiology and Neurobiology, Geisel School of Medicine, Dartmouth College, Lebanon, NH 03756

The PI 3-kinase (PI 3-K) signaling pathway is essential for Schwann cell myelination. Here we have characterized PI 3-K effectors activated during myelination by probing myelinating cultures and developing nerves with an antibody that recognizes phosphorylated substrates for this pathway. We identified a discrete number of phospho-proteins including the S6 ribosomal protein (S6rp), which is down-regulated at the onset of myelination, and N-myc downstream-regulated gene-1 (NDRG1), which is up-regulated strikingly with myelination. We show that type III Neuregulin1 on the axon is the primary activator of S6rp, an effector of mTORC1. In contrast, laminin-2 in the extracellular matrix (ECM), signaling through the α6β4 integrin and Sgk1 (serum and glucocorticoid-induced kinase 1), drives phosphorylation of NDRG1 in the Cajal bands of the abaxonal compartment. Unexpectedly, mice deficient in α6β4 integrin signaling or Sgk1 exhibit hypermyelination during development. These results identify functionally and spatially distinct PI 3-K pathways: an early, pro-myelinating pathway driven by axonal Neuregulin1 and a later-acting, laminin–integrin-dependent pathway that negatively regulates myelination.

Introduction

The myelin sheath is critical for the rapid and efficient conduction of nerve impulses in the vertebrate nervous system (Richie, 1984). Myelin forms in stages. In the developing peripheral nervous system (PNS), Schwann cells first segregate off large diameter axons into a 1:1 relationship, a process termed radial sorting (Feltri and Wrabetz, 2005; Sherman and Brophy, 2005). Subsequently, Schwann cells circumferentially extend a membrane process around the axon to form the myelin sheath (Bunge et al., 1989). In contrast, small-caliber axons remain ensheathed within separate pockets of a nonmyelinating Schwann cell, forming a Remak bundle (Griffin and Thompson, 2008).

The signals that direct Schwann cells to initiate myelination and regulate the thickness of the myelin sheath are incompletely understood (Pereira et al., 2012; Salzer, 2012). Two broad sources of extrinsic signals have been implicated in these events: axonal factors and components of the ECM. In particular, the type III isoform of Neuregulin1 on the axon surface and laminin-2 in the basal lamina are required for Schwann cells to segregate and myelinate axons properly (Bunge et al., 1986; Nave and Salzer, 2006). In addition to these major extrinsic signals, several additional signals have also recently been implicated in Schwann cell development (Glenn and Talbot, 2013).

These signals activate distinct receptors and signaling pathways. Neuregulin1 binds to the erbB2 and erbB3 coreceptors on

Correspondence to James L. Salzer: james.salzer@nyumc.org

Abbreviations used in this paper: α-DG, α-dystroglycan; MBP, myelin basic protein; mTor, mammalian target of rapamycin; NDRG1, N-myc downstream–regulated gene-1; P0, myelin protein zero; PI 3-K, phosphatidylinositol 3-kinase; PNS, peripheral nervous system; p-Sub; phospho-substrate; PTEN, phosphatase and tensin homologue; S6rp, S6 ribosomal protein; Sgk, serum and glucocorticoid-induced kinase; SLI, Schmidt Lanterman incisures.

The Rockefeller University Press $30.00
J. Cell Biol. Vol. 204 No. 7 1219–1236
www.jcb.org/cgi/doi/10.1083/jcb.201307057

the inner (i.e., the adaxonal) Schwann cell membrane (Canoll et al., 1996; Vartanian et al., 1997; Michailov et al., 2004). Neuregulin1-bound erbB2/3 activates PI 3-kinase (PI 3-K), among other pathways implicated in Schwann cell myelination (Maurel and Salzer, 2000; Kao et al., 2009; Newbern et al., 2011). In contrast, laminin receptors such as integrins and dystroglycan are present on the outer (i.e., the abaxonal) membrane (Einheber et al., 1993; Feltri et al., 1994; Saito et al., 2003). The α6β1 integrin has been shown to signal through Rac, focal adhesion kinase (FAK), and potentially integrin-linked kinase (ILK), in the radial sorting of axons before myelination (Feltri et al., 2002; Grove et al., 2007; Nodari et al., 2007; Pereira et al., 2009). As myelination proceeds, the α6β4 integrin and dystroglycan predominate and may function to stabilize myelin (Nodari et al., 2008). α6β4 can activate several downstream pathways including PI 3-K (Giancotti, 2007); the precise role of this integrin in mediating signaling in the PNS has not been examined.

In this study, we have focused on the PI 3-K pathway, which generates the signaling intermediates phosphatidylinositol biphosphate (PI-3,4-P2) and triphosphate (PI-3,4,5-P3) at the membrane (Cantley, 2002). PI 3-K activity is opposed by the lipid phosphatase and tensin homologue (PTEN), which hydrolyzes these phosphatidylinositols (Maehama and Dixon, 1998). The importance of this pathway in myelination is underscored by studies in which conditional ablation of PTEN in myelinating glia was shown to result in hypermyelination (Goebbels et al., 2010). Conversely, pharmacological inhibition PI 3-K signaling blocks myelination initiation (Maurel and Salzer, 2000).

Although PI 3-K is critical for myelination, its temporal activation and its various downstream effectors are incompletely characterized. Many signaling molecules in the PI 3-K pathway are activated by phosphatidylinositol-dependent kinase1 (PDK1), which binds PI-3,4-P2 and PI-3,4,5-P3 in the plasma membrane (Alessi et al., 1997a). Two well-described examples are Akt and Sgk (serum and glucocorticoid-induced kinase; Mora et al., 2004). These closely related serine–threonine kinase families both have three isoforms and share a substrate recognition motif (RXRXX*S/T) with each other and with the p70 and p90 ribosomal S6 kinases (Alessi et al., 1996; Kobayashi et al., 1999). Generation of antibodies against this sequence has facilitated investigations of the spatial and temporal expression of PI 3-K effectors (Kane et al., 2002; Kamimura et al., 2008).

Here we use this phospho-substrate antibody to characterize PI 3-K pathways and their effectors during myelination. Our findings support a model in which Neuregulin1 on the axon drives activation of Akt and thereby the mammalian target of rapamycin (mTOR) pathway in Schwann cells at the onset of myelination. Subsequently, laminin in the ECM activates Sgk1 via the α6β4 integrin, resulting in the phosphorylation of NDRG1 (N-myc downstream-regulated gene1), a Schwann cell phospho-protein critical for myelin stability (Kalaydjieva et al., 2000; Okuda et al., 2004). Phospho-NDRG1 is highly expressed in the Cajal bands of the abaxonal compartment, implicating these cytoplasmic channels as focal sites of integrin signaling. Unexpectedly, loss of either β4 integrin signaling or of Sgk1 enhances myelination during development. These results demonstrate a spatiotemporal progression of PI 3-K signaling from a pro-myelinating, Neuregulin1-dependent pathway to a laminin–integrin–Sgk1 pathway that negatively regulates PNS myelination.

Results

PI 3-K signaling substrates are distinctly regulated with myelination

To monitor the activity of the PI 3-K pathway during myelination, we used an antibody raised against the phosphorylated substrate recognition motif for a subset of AGC kinases (i.e., Akt, Sgk, p90 RSK, and p70 S6K; Zhang et al., 2002). We stained myelinating co-cultures of sensory neurons and Schwann cells with this antibody to localize putative PI 3-K substrates (Fig. 1). Every myelinating Schwann cell, identified by their expression of myelin basic protein (MBP), was robustly stained by the phospho-substrate (p-Sub) antibody along the length of the sheath. Phospho-substrates were also enriched in the Schmidt-Lanterman incisures (SLI; Fig. 1 C) and in the paranodes (Fig. 1 D), suggesting these regions are also foci of PI 3-K activity.

As all Schwann cells in these cultures were associated with axons but only myelinating Schwann cells were strongly stained, axonal contact is not sufficient to up-regulate these phospho-substrates. A subset of premyelinating Schwann cells that had elongated along the axon but expressed little if any MBP were also positively stained (Fig. 1 A, arrowheads in magnified insets). Premyelinating Schwann cells were identified by their expression of Oct-6/POU3F1, a transcription factor transiently up-regulated just before myelination (Fig. 1 B; Bermingham et al., 1996; Jaegle et al., 2003). Quantification of one set of cultures revealed that 10% (n = 154) of the premyelinating (POU3F1+/MBP−) cells were also stained by the p-Sub antibody. These results indicate that one or more phospho-substrates are up-regulated just before formation of compact myelin.

To further characterize the temporal expression of phospho-substrates, we used the p-Sub antibody to probe lysates from co-cultures that had myelinated for different times. These blots revealed a discrete number of bands (Fig. 2 A), most of which were up-regulated with myelination, indicated by increased myelin protein zero (P0) expression; this up-regulation is consistent with the increase in staining with the same antibody at the onset of myelination (Fig. 1 A). The most prominently up-regulated band is a doublet of ∼45 kD. In contrast, at least two phospho-proteins of ∼30 and ∼250 kD were down-regulated with myelination. Expression of these bands was also detected at lower levels in neuron-only and Schwann cell–only cultures, respectively (unpublished data).

These results suggest expression of these, and other phospho-proteins in Schwann cells, neurons, or both were altered as a consequence of axon–glial interactions. To determine if prolonged axon–Schwann cell interactions were sufficient to modulate their expression or myelination was required, we co-cultured Schwann cells and neurons together for 35 d in the presence or absence of ascorbate, which is required for myelination (Eldridge et al., 1987). We blotted the lysates with the p-Sub antibody, using p45 and p30 as representative substrates that are up-regulated and down-regulated, respectively (Fig. 2 B). Only the myelinated

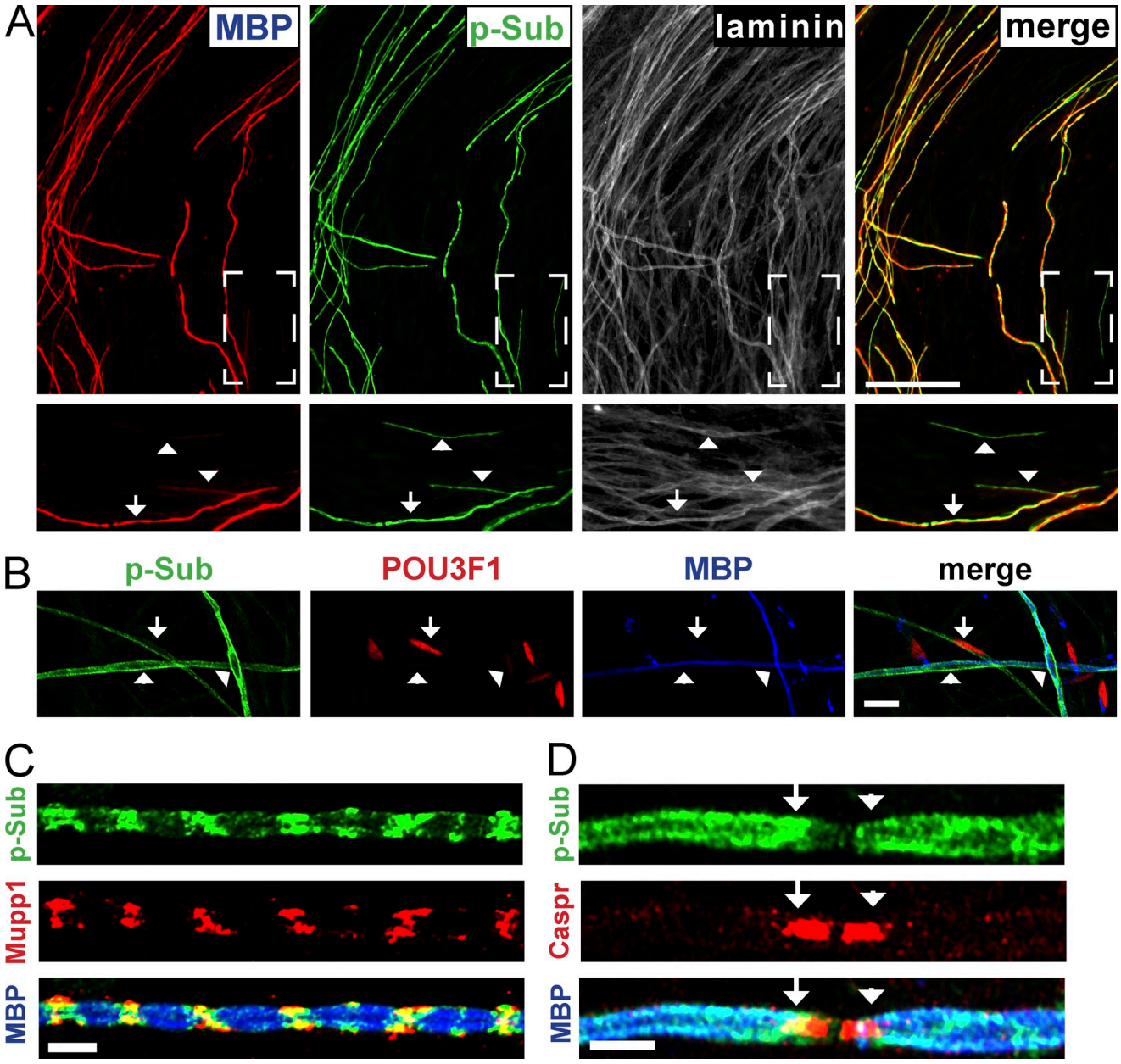

Figure 1. **Phospho-substrates are up-regulated with myelination.** (A) Myelinating co-cultures of rat sensory neurons and Schwann cells stained for MBP (red), p-Sub (green), and laminin (white); boxed areas are shown at higher magnification below at 1.5×. Myelinating Schwann cells (inset, arrow) are selectively stained with the phospho-substrate antibody (p-Sub). Some Schwann cells that have elongated but are not yet expressing MBP at significant levels are stained with the p-Sub antibody (arrowheads). Bar, 75 µm. (B) Staining of myelinating co-cultures for p-Sub (green), POU3F1 (red), and MBP (blue) is shown. A subset of premyelinating POU3F1-expressing Schwann cells coexpress phospho-substrates (arrow). All MBP-expressing Schwann cells, which are POU3F1-negative, coexpress phospho-substrates (arrowheads). Bar, 10 µm. (C) Myelinating co-cultures stained with p-Sub (green), Mupp1 (red), and MBP (blue) indicate that phospho-substrates are enriched in the SLI. Bar, 5 µm. (D) Myelinating co-cultures stained with p-Sub (green), Caspr1 (red), and MBP (blue) indicate that phospho-substrates are sometimes enriched in the distal glial paranode (arrow), extending into the juxtaparanode (arrowhead). Bar, 5 µm.

cultures exhibited the characteristic up-regulation of p45 and down-regulation of p30, suggesting that myelination regulates either their expression and/or their phosphorylation.

Identification of phospho-substrate proteins

To identify the p30 and p45 proteins, we took a candidate approach based on previous reports using the p-Sub antibody (Kane et al., 2002). We first examined whether p45 might correspond to phosphorylated N-myc downstream–regulated gene 1 (NDRG1), a protein of similar size that is phosphorylated at several sites, including Ser330 and Thr346/Thr356/Thr366 (3xThr; Murray et al., 2004). We used the p-Sub antibody to blot lysates from *stretcher* nerves, which express minimal levels of truncated NDRG1 and no full-length protein (King et al., 2011). p45 was undetectable in the *stretcher* nerve lysates (Fig. 3 A), confirming that this band corresponds to NDRG1. We also stained myelinating organotypic cultures prepared from wild-type and *stretcher*

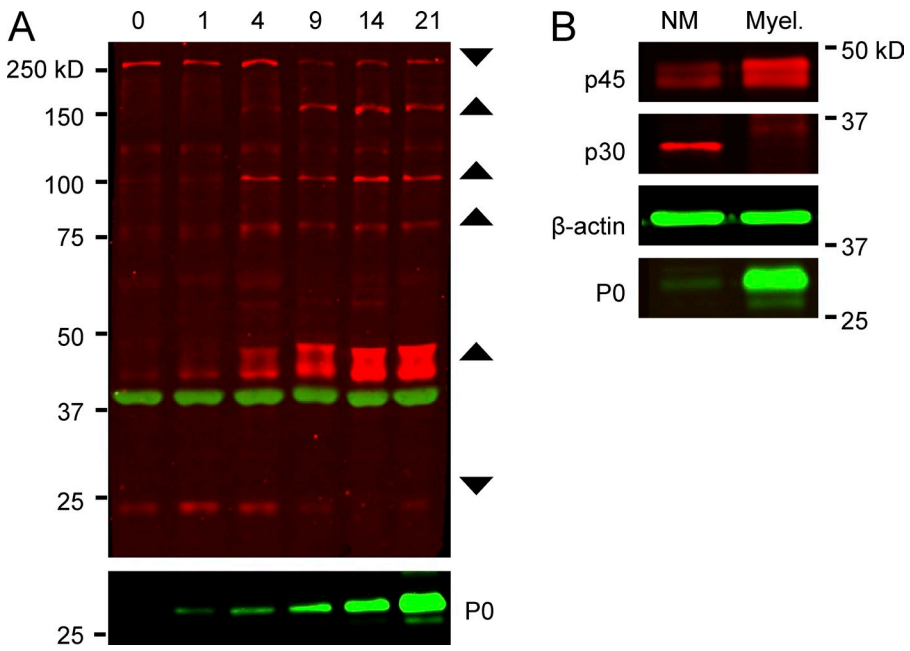

Figure 2. **Phospho-substrates are differentially expressed during myelination.** (A) Time course of the expression of phospho-substrates in myelinating co-cultures. Western blot analysis of lysates prepared from co-cultures beginning on day 0, when myelinating media was added, through day 21. Six major bands were detected that either increased or decreased as myelination proceeded. The p-Sub reactive bands are in red, β-actin in green; P0 myelin protein expression is also shown. (B) Co-cultures of Schwann cells and sensory neurons were maintained for 35 d under nonmyelinating (NM) or myelinating (Myel.) conditions. The increase in p45 and decrease in p30 observed in the time course shown in A only occur under myelinating conditions.

mice with the p-Sub and three NDRG1-specific antibodies (Berger et al., 2004; Sommer et al., 2013). We found that total and phospho-specific NDRG1 antibodies only stained the wild-type but not the *stretcher* cultures, indicating these antibodies are specific for NDRG1 (Fig. S1 A). In contrast, although staining of *stretcher* cultures with the p-Sub staining antibody was reduced, notably in the abaxon (Fig. S1 B), it was not abolished. These latter data show that NDRG1 is a major but not the only phosphorylated substrate in myelinating Schwann cells detected by the p-Sub antibody (Fig. 1 A).

We considered whether p30 is the S6 ribosomal protein (S6rp), a protein of similar molecular weight that is phosphorylated by S6 kinase and is downstream of Akt and mTOR signaling (Magnuson et al., 2012). We treated nonmyelinating co-cultures with inhibitors of PI 3-K (LY294002), mTor/TORC1 (rapamycin), and S6 kinase (PF4708671) for 18 h. Each inhibitor abolished p30 phosphorylation (Fig. 3 B), confirming that this band is p-S6rp.

Expression and localization of phospho-substrate proteins during myelination

We next examined the time course of Akt, S6rp, and NDRG1 phosphorylation during sciatic nerve development by Western blotting (Fig. 3 C). Based on Akt phosphorylation, PI 3-K is most active early in development and decreases as myelination proceeds. Phosphorylation of both Akt sites (i.e., T308, the PDK1 phosphorylation site, and S473, the TORC2 phosphorylation site; Alessi et al., 1997b; Sarbassov et al., 2005) is down-regulated with myelination. Similarly, S6rp is highly phosphorylated early and then down-regulated. The decrease in p-Akt and p-S6rp levels may also result from the decrease in total Akt and S6rp levels that accompanies myelination. In contrast, phospho- and total NDRG1 levels are robustly up-regulated with myelination. These data suggest that an early-acting PI 3-K pathway drives Akt and S6rp signaling and a late-acting PI 3-K pathway regulates NDRG1 phosphorylation, potentially independent of Akt.

To elucidate where in the Schwann cell these signaling events were localized, we stained myelinating co-cultures for p-Akt, p-S6rp, and p-NDRG1. The localization of p-Akt (S473) depended on the maturity of the myelin sheath (Fig. 4 A); it was initially localized along the length of the myelinating Schwann cell but concentrated at the paranodes as the sheath matured. Thus, at five days in myelinating media, premyelinating and nascent myelinating Schwann cells expressed p-Akt along the length of their processes. As myelination proceeded, p-Akt was localized to the paranodes of mature myelin sheaths, identified by expression of Caspr; p-Akt also was similarly localized in neonatal sciatic nerves (Fig. S1 C). This staining was specific, as it was lost when co-cultures were pretreated for 24 h with the PI 3-K inhibitor LY294002.

Staining of p-S6rp only partially overlapped with p-Akt. p-S6rp was most robustly expressed in nonmyelinating and 23% ($n = 172$) of premyelinating (POU3F1+/MBP−) Schwann cells (Fig. 4 B). Only a few MBP+ Schwann cells (3%) expressed p-S6rp, and these were weakly stained (an example is marked by an asterisk in Fig. 4 B). These data are consistent with Western blotting results showing that S6rp is down-regulated with myelination (Fig. 2 B and Fig. 3 C). The p-S6rp staining was present in the soma of premyelinating Schwann cells and in their processes that extended along and ensheathed neurites; no staining within neurites was detected.

Total and phosphorylated NDRG1 appeared to be enriched in the abaxon of myelinating Schwann cells (Fig. 4 C). Similar to p-Sub, we observed an occasional enrichment to the paranode in which p-Akt is localized. Taken together, these data suggest that p-Akt and p-S6rp are expressed at an early stage of axon–Schwann cell contact, whereas NDRG1 is downstream of a distinct pathway that is activated later in the abaxonal compartment.

To determine whether p-NDRG1 is indeed concentrated in the abaxonal compartment, we performed immunoelectron microscopy of myelinating co-cultures (Fig. S2, A and B). For immuno-EM, the numbers of gold particles in the abaxonal,

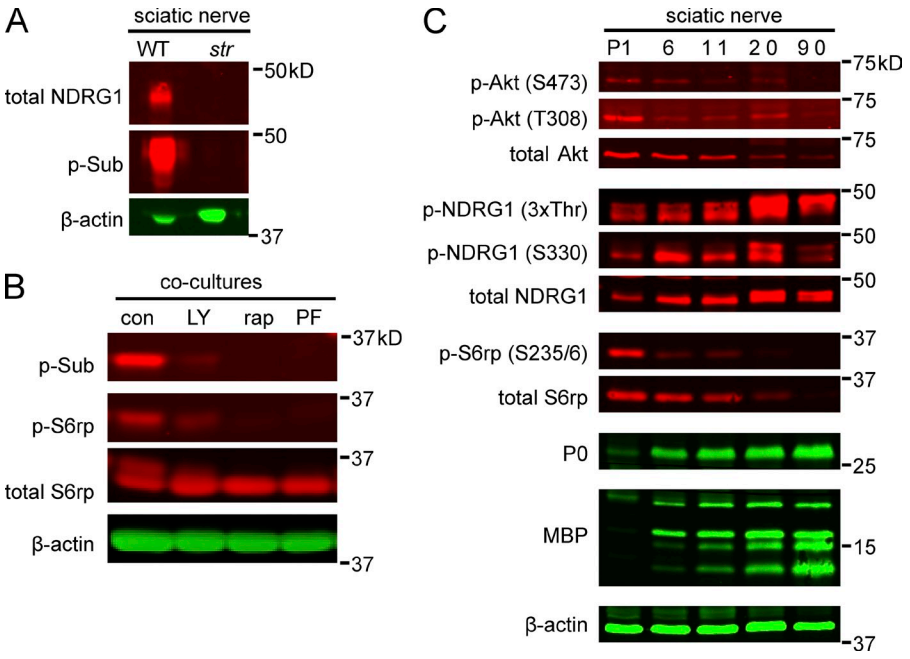

Figure 3. **S6rp and NDRG1 correspond to the 30- and 45-kD phospho-substrate bands.** (A) Western blots of wild-type and *stretcher* sciatic nerve lysates were probed with anti-NDRG1 and p-Sub antibodies; β-actin serves as a loading control. NDRG1 and the p45-kD p-Sub doublet are not detected in the *stretcher* nerve lysates. (B) Western blots of lysates from nonmyelinating co-cultures were treated with 50 nM rapamycin, 20 µM LY294002, or 40 µM PF-4708671 for 18 h and then probed with p-Sub, p-S6rp, and total S6rp antibodies. p-S6rp and p30 are not detectable in co-cultures treated with rapamycin, LY294002, or PF-4708671. (C) Expression of phospho- and total Akt, NDRG1, and S6rp in developing rat sciatic nerves. Lysates of postnatal sciatic nerves were probed on Western blots with the indicated antibodies. Both total and phosphorylated NDRG1 are up-regulated in parallel with compact myelin proteins P0 and MBP. S6rp and Akt are maximally expressed and phosphorylated early, then down-regulated as myelination proceeds.

adaxonal, and compact myelin compartments were determined in a blinded manner. Localization in each compartment was represented as a percentage of total particles counted in all three compartments. Myelin-associated glycoprotein and MBP served as controls for proteins expressed in the adaxon and in compact myelin, respectively. Analysis revealed more gold particles for phosphorylated NDRG1 (S330) in the abaxon than in compact myelin or the adaxon, supporting an abaxonal localization.

We also stained adult teased nerve fibers for total and p-NDRG1 (3xThr) and with antibodies to Necl–4, a marker of the Schwann cell periaxonal membrane and clefts (Maurel et al., 2007; Spiegel et al., 2007) and to α-dystroglycan (α-DG), a laminin receptor exclusive to the abaxonal Schwann cell membrane. Total NDRG1 was present in the adaxonal compartment, in the SLI, and in the abaxonal compartment (Fig. 5 A). In contrast, p-NDRG1 was present only in the outer aspect of the SLI and in the abaxonal compartment (Fig. 5 B); no adaxonal staining was observed. By imaging the surface of the nerve fibers (Fig. 5, C and D), we determined that both total and p-NDRG1 are enriched in the Cajal bands (i.e., the cytoplasmic channels that form between α-DG–positive appositions in the abaxonal compartment). Taken together, these data indicate that total and phosphorylated NDRG1 are enriched in the Cajal bands and clefts. Although total NDRG1 is present in the adaxonal compartment, as previously reported (Berger et al., 2004), it is not phosphorylated in this site.

S6rp is a substrate of Neuregulin1 type III signaling; NDRG1 is a substrate of laminin signaling

The distinct spatial and temporal patterns of p-S6rp and NDRG1 phosphorylation suggest that they are activated by different signals. We therefore compared substrate phosphorylation of NDRG1 and S6rp in two in vivo mouse models: (1) Neuregulin1 type III haploinsufficient mice ($Nrg1^{+/-}$), and (2) laminin-2–null (dy^{3k}/dy^{3k}) mice (blots shown in Fig. 6 A, quantification in Fig. 6 B). Nerves were analyzed at P10 when both NDRG1 and S6rp are normally robustly phosphorylated (Fig. 3 C). Mice haploinsufficient for type III Neuregulin1, which are known to be hypomyelinated (Michailov et al., 2004; Taveggia et al., 2005), had reduced levels of p-Akt (T308) and of p-S6rp but normal levels of p-NDRG1. Similarly, p-S6rp is virtually undetectable in Schwann cells co-cultured under myelinating conditions with Neuregulin1 type III–null sensory neurons relative to their wild-type counterparts (Fig. S2 C). In contrast, p-NDRG1 was decreased dramatically in the dy^{3k}/dy^{3k} mice, in addition to a modest reduction in p-S6rp levels. Thus, S6rp phosphorylation is driven by Neuregulin1 and potentially by laminin, whereas NDRG1 phosphorylation is primarily laminin dependent.

NDRG1 phosphorylation is dependent on laminin receptors

These data indicate laminin is necessary for NDRG1 phosphorylation. To determine whether it is also sufficient, we applied laminin, with or without the LY inhibitor, for 30 min to serum-starved cultures of pure Schwann cells or co-cultures of Schwann cells and sensory neurons (Fig. S3, A and B). Addition of laminin resulted in robust NDRG1 phosphorylation only in Schwann cells co-cultured with neurons; there was no increase when laminin was added to Schwann cells cultured alone. The application of soluble Neuregulin1 type III also up-regulated NDRG1 phosphorylation in nonmyelinating cultures, suggesting that signaling is not compartmentalized before the formation of the abaxon and adaxon (Fig. S3 C). These data indicate that the signaling pathway(s) that drive NDRG1 phosphorylation downstream of laminin require axonal contact.

We next examined the role of Schwann cell laminin receptors in transducing the phosphorylation signal, focusing on the α6β1 and α6β4 integrins. Both integrins are expressed on the abaxonal membrane of Schwann cells; α6β4 expression is axon

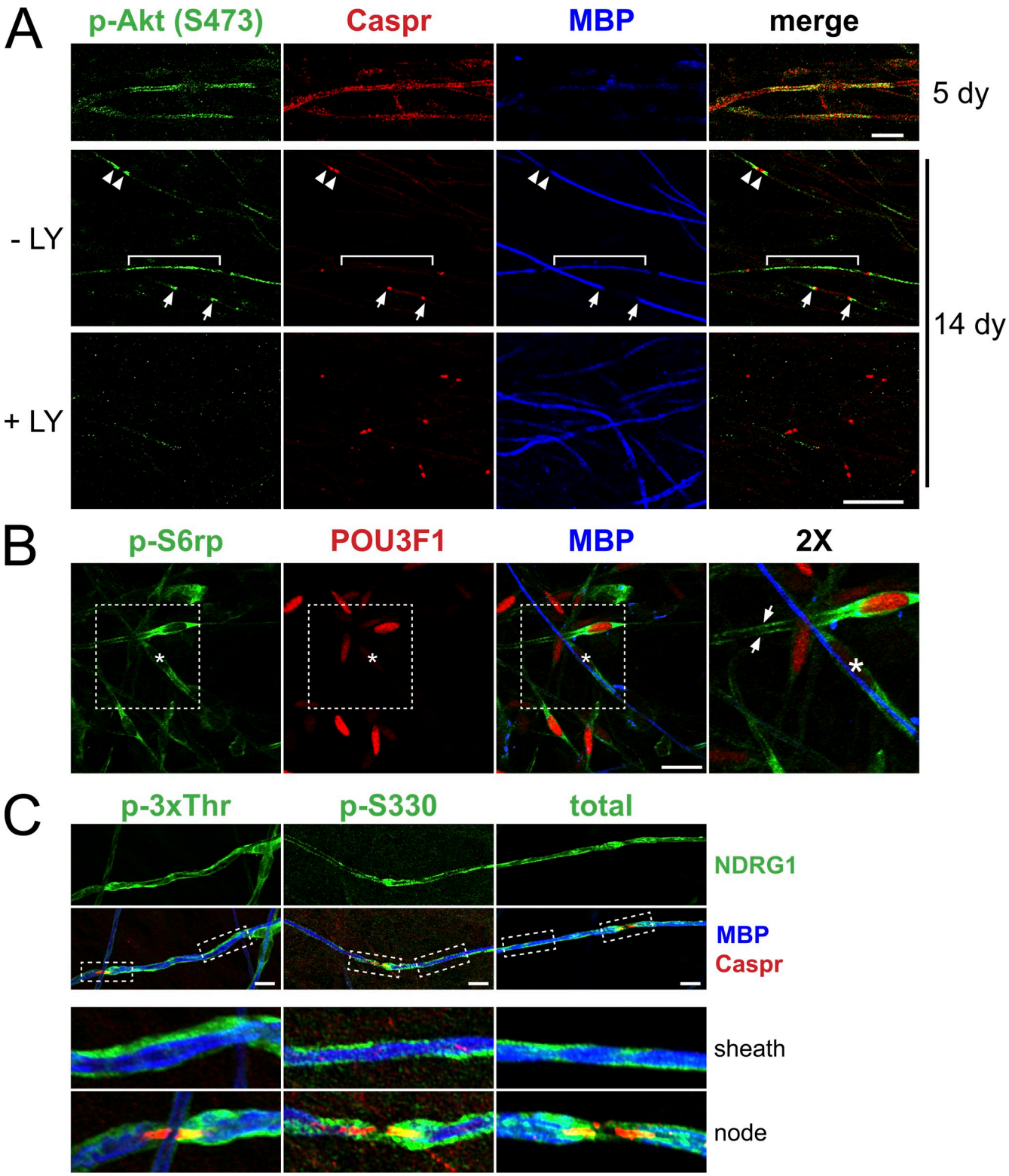

Figure 4. **Localization of p-S6rp, p-NDRG1, and p-Akt in myelinating co-cultures.** (A) Co-cultures maintained in myelinating media for 5 or 14 d were stained for p-Akt (green), Caspr (red), and MBP (blue). In 5-d co-cultures (top row), Schwann cells just before myelinating express p-Akt (S473) along their length; Caspr staining of axons is diffuse and MBP is not yet expressed. In 14-d co-cultures (bottom two rows), p-Akt staining varied depending on the maturity of the myelin segments. In a thinly myelinated segment with a single paranode (bracket), p-Akt was prominent along the Schwann cells, in more mature segments with two hemi-paranodes (arrows) or surrounding a mature node (arrowheads) staining was concentrated in the paranodal and juxtaparanodal regions. Addition of the LY inhibitor before fixation abolished p-Akt staining. Bar, 20 µm. (B) Myelinating co-cultures were stained for p-S6rp (green), POU3F1 (red), and MBP (blue). p-S6rp was maximally expressed in the cytoplasm and along the processes of a premyelinating Schwann cell expressing POU3F1 (arrows) and at lower levels in myelinated Schwann cells (one is marked by an asterisk). Bar, 20 µm. Inset (far right panel) is at 2×. (C) Myelinating co-cultures stained for phospho- (3xThr, S330) and total NDRG1 (all green), MBP (blue), and Caspr (red). Myelinating Schwann cells express phospho- and total NDRG1 (green) along the outside of the myelin sheath and in some paranodes (insets, 3× magnification). Bar, 20 µm.

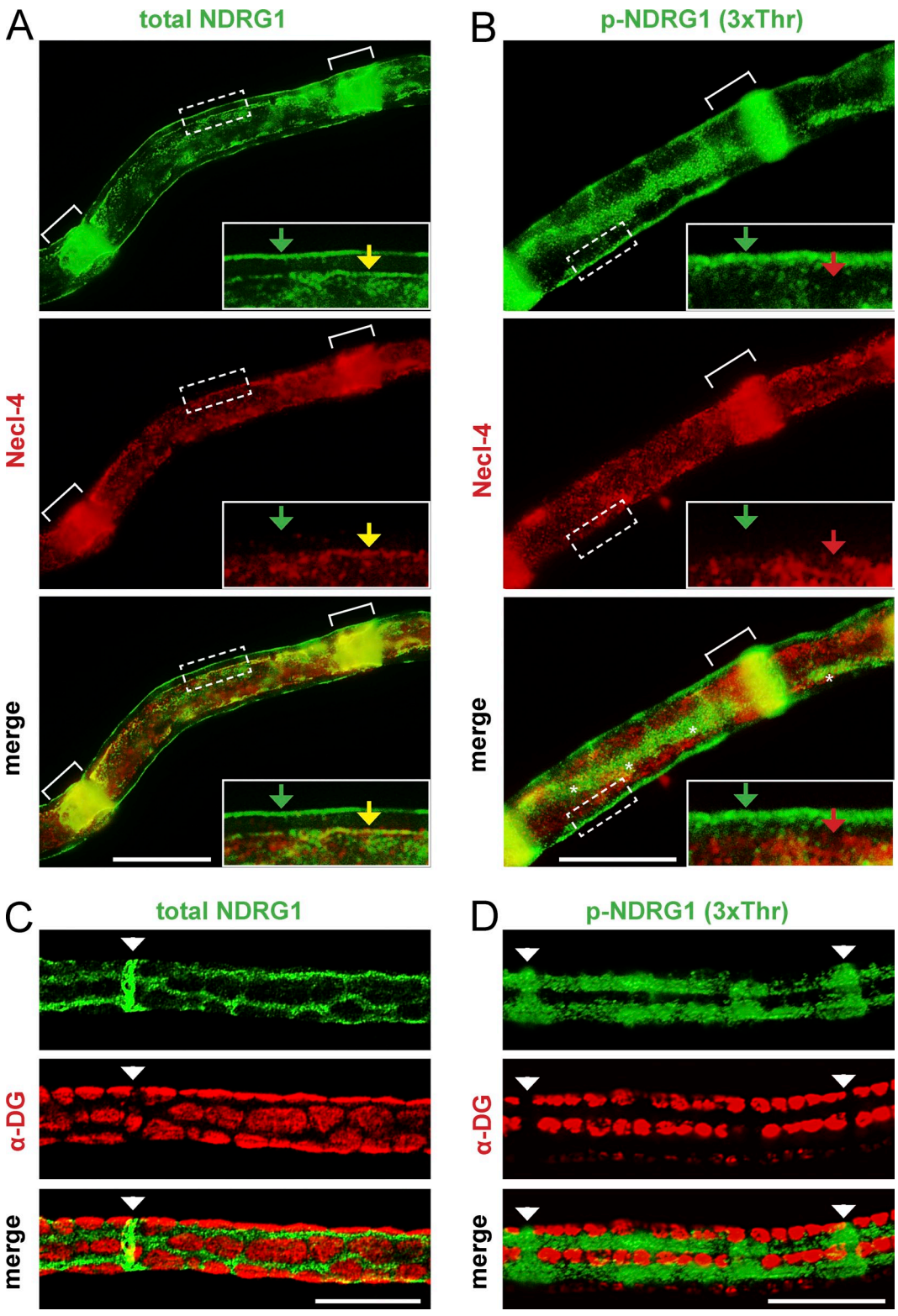

Figure 5. **NDRG1 is enriched in the Cajal bands of the abaxonal compartment.** (A) A teased adult rat sciatic nerve fiber stained for total NDRG1 (green) and Necl-4 (red) is shown. Total NDRG1 is present in the abaxon (green arrow), adaxon (yellow arrow), and throughout the length of the SLI (white brackets); Necl-4 is present in the adaxonal membrane and the incisures. Inset is rotated and shown at 3×. Bar, 20 µm. (B) Teased adult rat sciatic nerve fiber stained for phospho-NDRG1 (green) and Necl-4 (red) is shown. p-NDRG1 is expressed in the abaxon (green arrow) but not the adaxon (red arrow) and only the outer portion of the SLI (white brackets). Necl-4 is expressed throughout the entire incisures. A Cajal band is present in the center of the fiber (white asterisks). Inset is rotated and shown at 3×. Bar, 20 µm. (C and D) Teased P45 mouse sciatic nerve fibers stained for (C) total or (D) p-NDRG1 (green) and α-dystroglycan (red); SLI are labeled with white arrowheads. Both total and p-NDRG1 are enriched in the Cajal bands and excluded from the α-DG stained appositions. Bar, 20 µm.

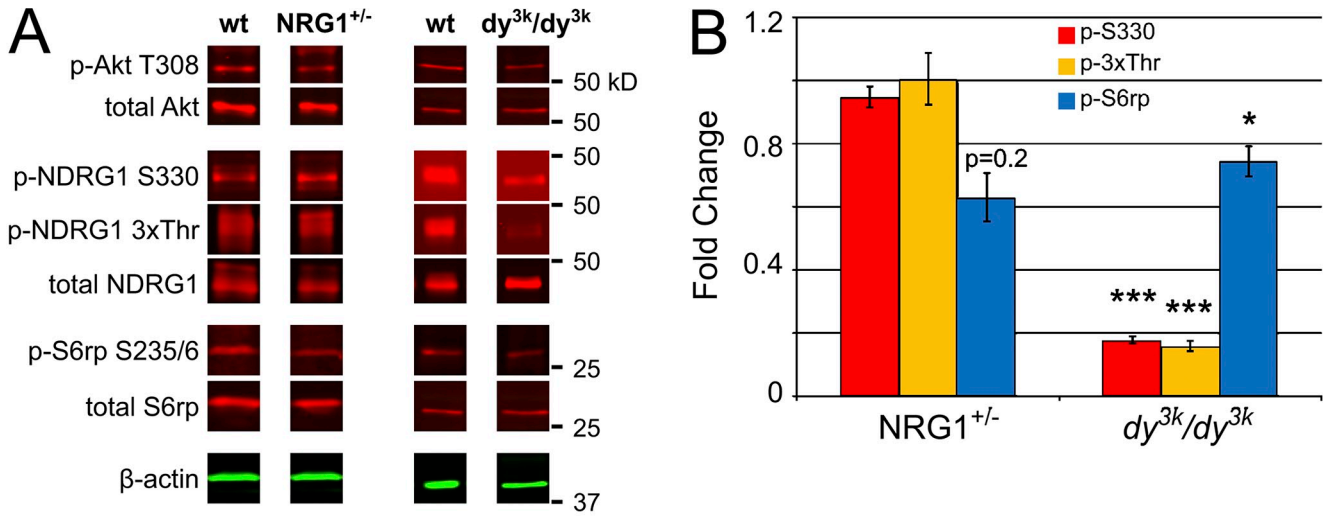

Figure 6. **Neuregulin1 and laminin-2 differentially regulate S6rp and NDRG1 phosphorylation.** (A) Lysates of P10 nerve from Neuregulin1 type III haploinsufficient or α2-laminin–null (*dy*^{3k}/*dy*^{3k}) mice were blotted for total and phosphorylated Akt, S6rp, and NDRG1. Whereas p-Akt is reduced in both nerves, phospho-NDRG1 is markedly reduced only in the α2-laminin–null mice. (B) Quantification of the phosphoprotein levels in neuregulin and laminin mutant nerves are shown normalized to total protein in each case. Mean ± SEM; *, P < 0.05; ***, P < 0.001 by two-tailed Student's *t* test; $n \geq 3$.

contact dependent and up-regulated with myelination in a pattern similar to that of NDRG1 phosphorylation; β1 persists during myelination but is maximally expressed before myelination and by Schwann cells cultured alone (Einheber et al., 1993; Feltri et al., 1994). Floxed alleles of the β1 and β4 integrin subunits, and of α-DG were conditionally ablated in Schwann cells beginning at E15 using the P0 Cre driver line (Feltri et al., 1999). Nerves from the P0 Cre driver line served as a control.

We analyzed NDRG1 phosphorylation in lysates of P10 nerves deficient in each of these laminin receptors (Fig. 7 A and Fig. S4 A). Nerves deficient in α-DG exhibited a modest reduction of NDRG1 phosphorylation at both sites. A more significant reduction was observed in the β1 and β4 integrin conditional nulls but only at Ser330. This latter result suggests that there may be compensatory mechanisms in the integrin nulls that rescue downstream signaling of the p-3xThr site. To test this possibility, we examined a loss-of-function knock-in mouse model in which β4 integrin is missing its canonical signaling domain; this mutant is expressed at physiological levels, heterodimerizes with the α6 subunit, and binds to laminin properly (Nikolopoulos et al., 2004). NDRG1 phosphorylation was significantly reduced at both sites in the β4 integrin signaling mutant. These data suggest that there are cooperative effects of laminin receptors in promoting NDRG1 phosphorylation, with a key role of β4 integrin in transducing the laminin signal to NDRG1. Importantly, phosphorylation of S6rp is not significantly reduced in the β4 integrin–signaling mutant (Fig. 7 B and Fig. S4 B) indicating its phosphorylation is distinctly regulated from NDRG1 and is not primarily downstream of matrix–integrin interactions.

Akt1 and Sgk1 contribute to NDRG1 phosphorylation

To determine the kinases downstream of β4 integrin, and other laminin receptors, that phosphorylate NDRG1 we took a candidate approach. Sgk1 has been proposed to be the primary NDRG1 kinase, although recent data suggest that Akt may also play a role (Burchfield et al., 2004; Murray et al., 2004; Sommer et al., 2013). We therefore examined NDRG1 phosphorylation in P10 and adult knockout nerves from Sgk1- and Sgk3-null animals; these two Sgk isoforms are the sole isoforms expressed in Schwann cells based upon RT-PCR analysis (Fig. 8 A). We found a major reduction in NDRG1 phosphorylation at the 3xThr sites in the Sgk1 knockout nerves at P10 and at all sites (S330, 3xThr) in the adult (Fig. 8 B and Fig. S4 C). Sgk3 knockout nerves also showed a reduction of phosphorylation at the 3xThr sites. These data provide strong support for an important but not an exclusive role of Sgk1 in NDRG1 phosphorylation.

Because phosphorylation at S330 was not reduced in either Sgk-null mice at P10, we examined NDRG1 phosphorylation in the Akt1, 2, and 3 knockout nerves (Fig. S4 D). Loss of Akt1, but not of Akt2 or 3, decreased p-S330 but not p-3xThr. Therefore, both Akt1 and Sgk1 contribute to NDRG1 phosphorylation during development, whereas Sgk1 and Sgk3 are the major NDRG1 kinases in the adult.

Loss of β4 integrin signaling and Sgk1 enhance myelination during development

These studies suggest that Sgk1 is an important regulator of NDRG1 phosphorylation in myelinating Schwann cells. Although Sgk1-null mice develop normally and do not exhibit any overt neurological phenotype, the role of Sgk1 in myelination has not been specifically examined (Wulff et al., 2002; Fejes-Tóth et al., 2008). To address its function in myelination directly, we analyzed P10 sciatic nerve from Sgk1-null, heterozygous, and wild-type siblings by EM (Fig. 9). Sgk1-null nerves appeared normal, but on close inspection exhibited thicker myelin sheaths on average than their wild-type littermates (Fig. 9 A). This was confirmed by the reduced g-ratios in the knockout mice, in which there is a dose-dependent effect of Sgk1 as heterozygotes had g-ratios intermediate between wild-type

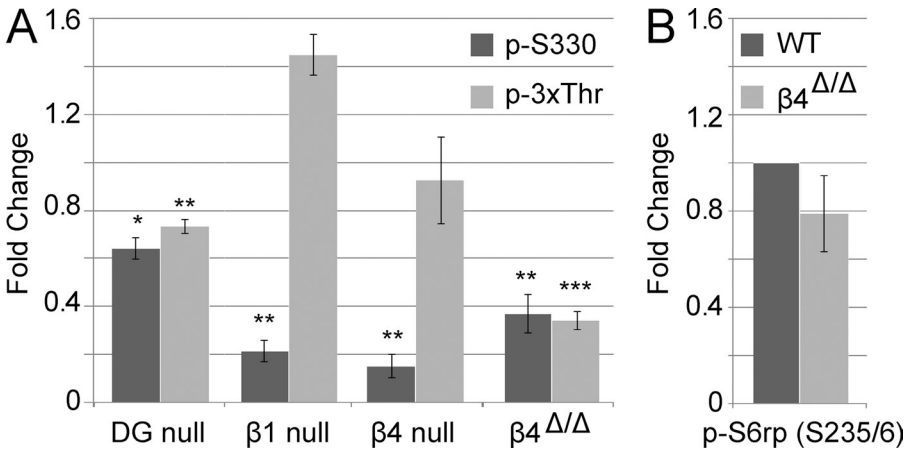

Figure 7. **β4 integrin is a key laminin receptor upstream of NDRG1 phosphorylation.** (A) Lysates from P10 nerves deficient in various laminin receptors were probed for alterations in NDRG1 phosphorylation at the p-S330 and p-3xThr sites. p-NDRG1 levels are normalized to total NDRG1 for each quantification. Conditional ablation of the β1 ($n = 3$) and β4 ($n = 4$) integrin subunit causes a defect on S330 phosphorylation but not p-3xThr. The signaling-defective β4 mutant ($\beta4^{\Delta/\Delta}$; $n = 7$) exhibits a marked reduction of phosphorylation at both the S330 and 3xThr sites. The DG-null has a small but significant defect at both S330 and 3xThr ($n = 5$). Mean ± SEM; *, $P \leq 0.05$; **, $P < 0.01$; ***, $P < 0.001$ by two-tailed *t* test. (B) P10 β4-signaling mutant nerves have normal levels of S6rp phosphorylation. Quantifications were normalized to total S6rp protein levels. Mean ± SEM; $n = 4$; $P > 0.05$ by two-tailed *t* test.

and knockout nerves (Fig. 9 E). This effect is most evident in small- and medium-caliber axons (Fig. 9 F).

Additional abnormalities observed in the Sgk1 nulls included more complete sorting of larger-caliber axons compared with controls. Thus, there were 15 unsorted axons larger than 1.1 µm in diameter among the 50 fields of wild-type nerves examined (Fig. 9 B); all axons of this size were sorted in 50 fields of Sgk1 nulls. There were also twice as many smaller-caliber axons (i.e., less than 0.9 µm in diameter) that were myelinated in the Sgk1 nulls relative to the wild types, and these tended to be hypermyelinated ($P > 0.05$). Finally, we also observed examples of polyaxonal myelination, i.e., multiple small-caliber axons that were myelinated in common by a single Schwann cell, in the Sgk1 nulls (Fig. 9 C); none were observed in the wild-type or heterozygote mice. No abnormalities of Remak fibers were observed in the nulls, indicating the defects are specific to myelinated fibers. Taken together, these findings indicate that radial sorting is accelerated and myelin sheath thickness increased in Sgk1-null nerve at P10, implicating Sgk1 as a negative regulator of myelination during early development.

Because Sgk1 signals downstream of α6β4, we also examined myelination in the β4-signaling mutant mice. These mice also demonstrated modest hypermyelination (Fig. 9 D; quantified in Fig. S5 A), which was most evident in fibers of medium diameter (1.5–2.5 µm).

Taken together, these results unexpectedly implicate integrin signaling from the matrix via PI 3-K/Sgk1 as an inhibitor of myelination. Several proteins have been identified as negative regulators of PI 3-K/Akt signaling (i.e., DLG1, PTEN, and REDD1; Cotter et al., 2010; Noseda et al., 2013). We therefore examined whether their expression was altered in Sgk1-null nerves (Fig. S5 B). We found that none of these molecules were significantly altered. Whereas REDD1 levels were modestly reduced, mTOR activity (indicated by p-S6rp levels), its negatively regulated effector, was not consistently increased. These results suggest that the mechanism(s) by which β4 integrin and Sgk1 down-regulate myelination may involve other signaling pathways.

Discussion

Schwann cell myelination depends on a discrete number of extrinsic signals originating from the axon and the ECM (Pereira et al., 2012; Salzer, 2012; Glenn and Talbot, 2013). These signals, in turn, activate a complex set of intracellular pathways. Elucidating the effectors of these pathways, and determining the sites where they act, will be essential to an understanding of how these ligands and pathways cooperate to promote myelin assembly. Here, we have characterized further the PI 3-K pathway during myelination. Our studies indicate that PI 3-K is transiently activated by Neuregulin1 at the onset of myelination, driving the Akt/mTOR pathway; subsequently, PI 3-K is activated by laminin as the sheath matures, activating Sgk1 and inhibiting myelination (Fig. 10). Our data further suggests these pathways are spatially segregated. These findings are considered further below.

Neuregulin1 signaling is the main activator of mTOR at the onset of myelination

We previously demonstrated that type III Neuregulin1 is the key signal on the axon that activates PI 3-K, which in turn is essential for myelination (Maurel and Salzer, 2000; Taveggia et al., 2005). Here we demonstrate that type III Neuregulin1 on the axon is also the major driver of TORC1 activation, based on p-S6rp levels. During initial interactions, p-Akt is present along the length of the elongated, premyelinating Schwann cells (Fig. 4 A) in direct apposition to the axon and thus Neuregulin1. Similarly, p-S6rp is present in the ensheathing processes of premyelinating Schwann cells (Fig. 4 B). p-S6rp levels are activated in concert with p-Akt and well before the peak of laminin signaling indicated by NDRG1 phosphorylation (Fig. 3 C). Finally, genetically reducing or ablating Neuregulin1 in vivo and in vitro resulted in reduced activation of p-Akt and p-S6rp (Fig. 6 and Fig. S2 C).

There may also be a modest, supplemental role of laminin–integrin signaling in the activation of PI 3-K/Akt/mTOR in myelinating Schwann cells. p-S6rp levels are somewhat reduced in laminin-deficient mice at P10 (Fig. 6). This may be a direct effect

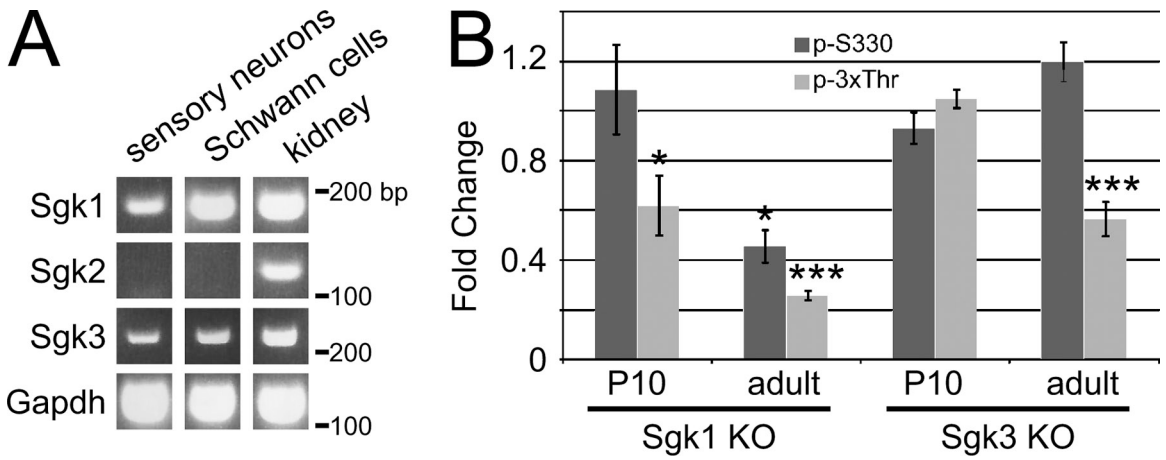

Figure 8. **Sgk isoforms phosphorylate NDRG1.** (A) RT-PCR of first-strand cDNA obtained from pure sensory neurons, Schwann cells, and kidney (control) using Sgk isoform-specific primers demonstrates Sgk1 and Sgk3 are expressed by Schwann cells. (B) Quantification of Western blots analyzing phosphorylation at the p-S330 and 3xThr sites of NDRG1 in P10 and adult (~P60) sciatic nerves from Sgk1- or Sgk3-specific knockouts. Sgk1 loss of function reduces NDRG1 phosphorylation at the 3xThr site at P10 and at both sites in the adult. Sgk3 loss of function slightly increases p-S330 and decreases 3xThr in the adult. p-NDRG1 was normalized to total NDRG1, which was similar across phenotypes, for the quantification. Mean fold change relative to wild type ± SEM, $n \geq 4$. *, $P < 0.05$; ***, $P < 0.001$ by two-tailed Student's *t* test.

of laminin or, alternatively may reflect its role in promoting Schwann cell ensheathment of axons and thereby erbB receptor phosphorylation and PI 3-K/Akt/mTOR activation (Yu et al., 2005; Berti et al., 2011). The former possibility is suggested by the slight reduction of p-S6rp in the β4 integrin–signaling mutant at P10 (Fig. 7 B), although this did not reach statistical significance. In addition, p-S6rp is detected at low levels in the soma of some myelinating Schwann cells (Fig. 4 B) in culture and in the adult mouse (Sherman et al., 2012), consistent with direct activation in the abaxonal compartment downstream of laminin. Taken together, these data indicate that Neuregulin1 on the axon is the major regulator of S6rp phosphorylation and TORC1 activity during development; however, once myelination is complete, laminin signaling may contribute to low-level activation.

mTOR has a key role during PNS myelination based on conditional knockouts of mTOR in embryonic Schwann cells, which exhibit thin, short myelin sheaths (Sherman et al., 2012). These results further implicate the Neuregulin1/PI 3-K/Akt/mTOR pathway in the radial and longitudinal expansion of the myelin sheath. They also suggest that the hypomyelination observed in mice haploinsufficient for Neuregulin1 (Michailov et al., 2004; Taveggia et al., 2005) likely results, in part, from reduced mTOR activity. The precise role(s) of mTOR during myelination remains to be established but may reflect its key role in regulating protein translation (Laplante and Sabatini, 2013), potentially including translation of proteins required for myelination. Indeed, the expression of p-S6rp in ensheathing processes (Fig. 4 B) is appropriately localized to regulate local translation at the onset of myelin biosynthesis.

Spatiotemporal changes in PI 3-kinase signaling during myelination

As myelination proceeds, PI 3-K activity progressively decreases (Fig. 3 C), including along the internode (Fig. 4 A). This reduction is consistent with the limited effects of inhibiting PI 3-K after myelination is established (Maurel and Salzer, 2000) and of ablating Neuregulin1 and erbB2 in the adult (Atanasoski et al., 2006; Fricker et al., 2009). Thus, although activation of PI 3-K by Neuregulin1 is critical for the initial events of myelination, it is dispensable for myelin maintenance. The decline in p-Akt activity along the internode may be multifactorial. One mechanism is the recruitment of PTEN to the adaxonal compartment, where it interacts with and is likely stabilized by DLG1 (Ozçelik et al., 2010; Sandoval et al., 2013). In addition, we have found that total Akt levels are substantially down-regulated during myelination (Fig. 3 C), likely further limiting signaling.

The reduction of p-Akt along the internode is accompanied by its enrichment within the paranodes in vitro and in vivo during active myelination (Fig. 3 C, Fig. 4 A, and Fig. S1 A). Enrichment of p-Akt in the paranodes was also observed in PTEN-conditional mice, which exhibit markedly elevated PI 3-K activity (Goebbels et al., 2010), and is consistent with localization of phospho-substrates at this site (Fig. 1 D). Akt may be activated in the paranodes as the result of converging signals from adaxonal erbB receptors and abaxonal laminin receptors. In addition, the autotypic adherens junctions, which form between the paranodal loops themselves, may be another source of PI 3-K activity (Fannon et al., 1995; Rivard, 2009). Enrichment of phospho-substrates in the SLI (Fig. 1 C and Fig. 5) further supports the clefts as a locus of PI 3-K signaling.

Phospho-NDRG1 localization implicates Cajal bands as sites of laminin and α6β4 integrin signaling

Both total and p-NDRG1 are dramatically up-regulated with myelination (Fig. 3 C), consistent with a previous report (Berger et al., 2004). These authors also reported that NDRG1 is expressed throughout the Schwann cell cytoplasm. Here, we show both total and p-NDRG1 are strikingly enriched in the Cajal bands, providing compelling evidence that NDRG1 is concentrated abaxonally (Fig. 5 B). The Cajal bands are anastomosing

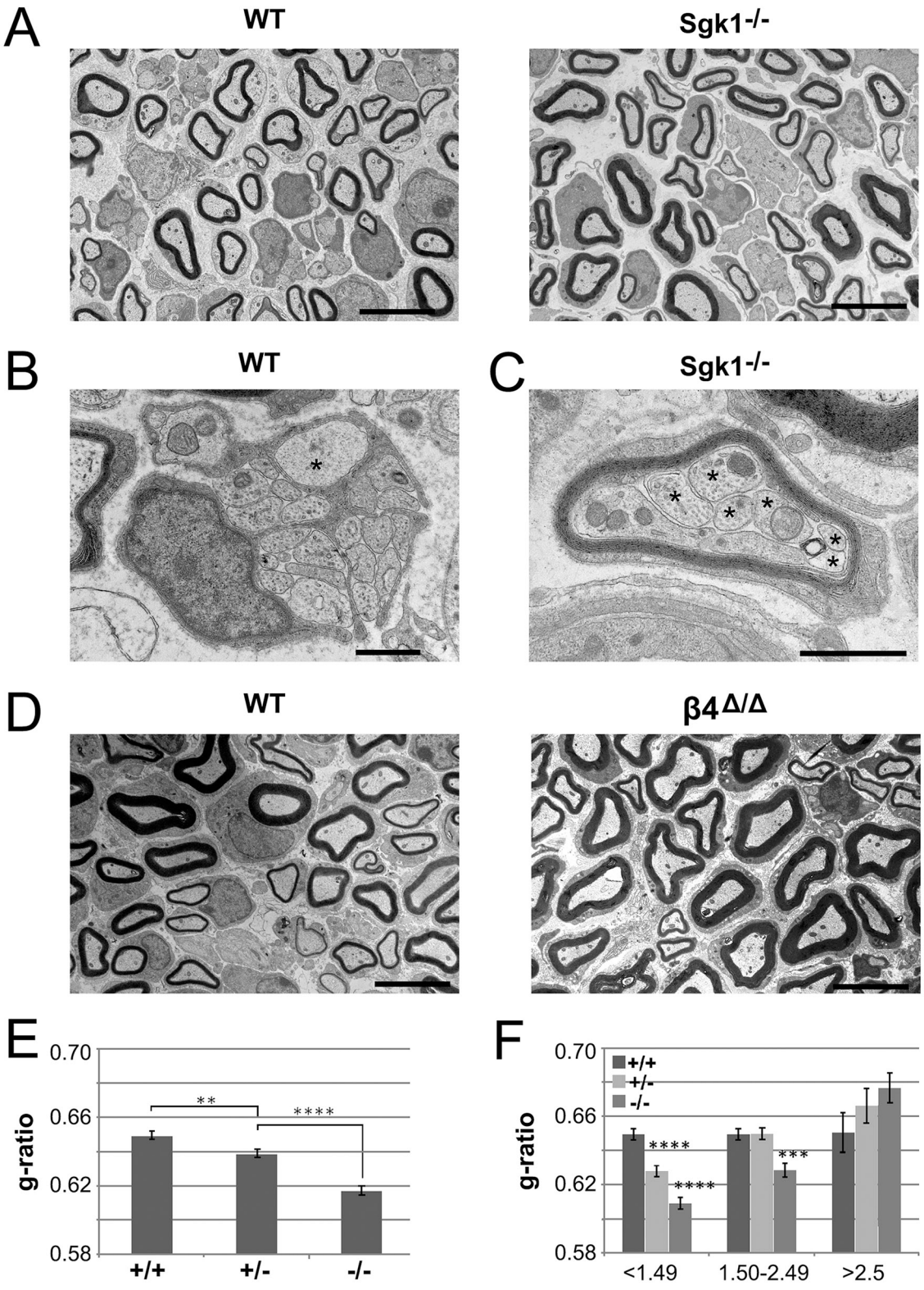

Figure 9. **Sgk1-null mice are hypermyelinated during development.** (A) Representative electron microscopic fields of P10 nerves from wild-type and *Sgk1*$^{-/-}$ mice are shown, demonstrating modest hypermyelination of some fibers in the null nerve. Bars, 5 µm. (B) At P10, large-caliber axons (asterisk) are still occasionally ensheathed in the Remak bundles of wild-type but not Sgk1 knockout nerves (not depicted). Bar, 1 µm. (C) An example of multiple small axons (asterisks) communally myelinated by a single Schwann cell from the Sgk1-null mice is shown. Bar, 1 µm. (D) Representative electron microscopic fields of P10 nerves from wild-type and β4-signaling mutant mice are shown, demonstrating modest hypermyelination of some fibers in the mutant nerve. Bars, 5 µm. (E) Quantification of the g-ratios in P10 nerves from wild-type (884 axons scored), *Sgk1*$^{+/-}$ (942 axons scored), and *Sgk1*$^{-/-}$ (796 axons scored) mice. Loss of Sgk1 results in a modest hypermyelination that is dose dependent. Mean g-ratios are shown ± SEM; **, $P < 0.01$; ****, $P < 0.0001$ by ANOVA. (F) Quantification of the g-ratios in P10 nerves from wild type, *Sgk1*$^{+/-}$, and *Sgk1*$^{-/-}$ binned by axon caliber. Mean g-ratios are shown ± SEM; ***, $P < 0.001$; ****, $P < 0.0001$ by ANOVA and Tukey's multiple comparisons test.

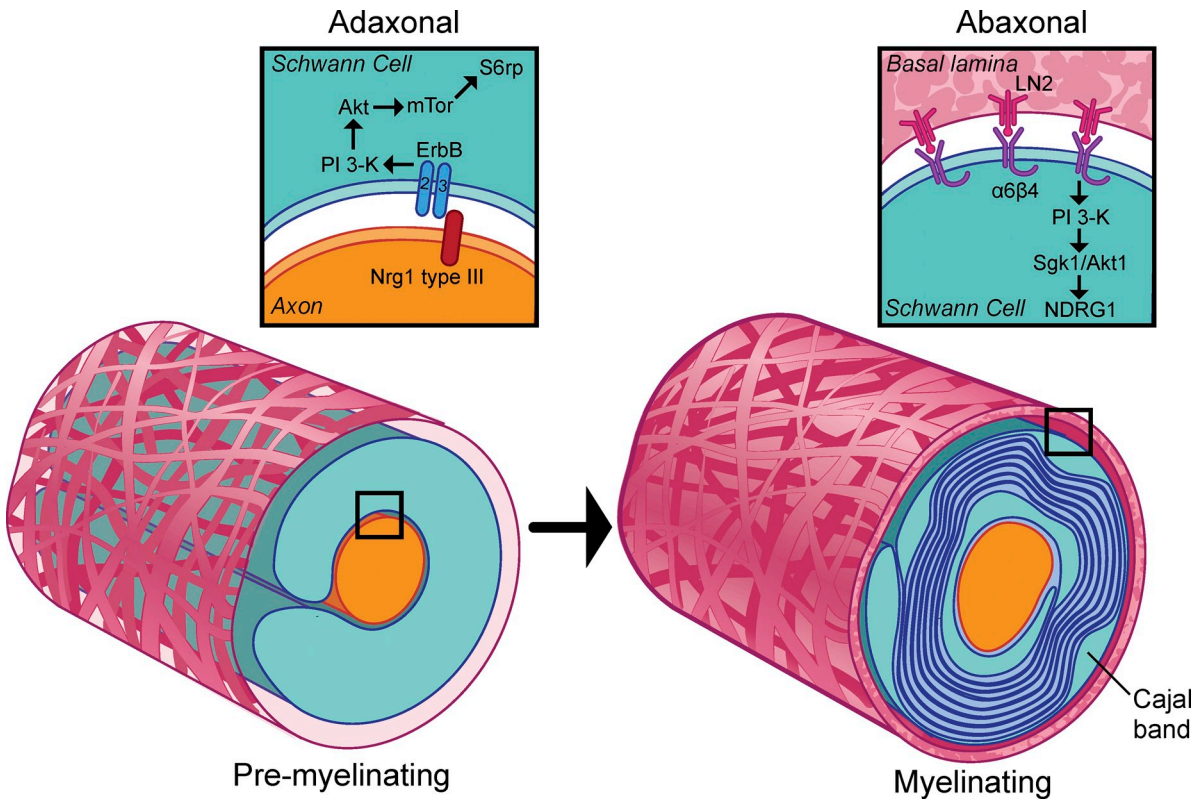

Figure 10. **Schematic of PI 3-K pathways activated during myelination.** Schematic of the proposed transition in PI 3-K during myelination. In premyelinating Schwann cells (left), Neuregulin1 drives myelination by activating TORC1 through erbB-dependent PI 3-K/Akt activation. In myelinating Schwann cells (right), pro-myelinating signals are opposed by laminin signaling via α6β4 integrin and Sgk1. This signaling is localized to the Cajal bands of the abaxon; among the targets of Sgk1 phosphorylation is NDRG1, a protein required for long-term myelin maintenance.

cytoplasmic channels interposed between α-DG–positive appositions that form between the outer Schwann cell membrane and the compact myelin sheath (Sherman and Brophy, 2005). Although their precise function is not known, the Cajal bands are thought to provide a conduit for the centrifugal transport of proteins and RNA from the perinuclear region (Gould and Mattingly, 1990; Court et al., 2004).

This abaxonal localization is consistent with the dependence of NDRG1 phosphorylation on laminin-2 and laminin receptor signaling. Both β1 and β4 integrins contribute to the PI 3-K signaling upstream of NDRG1 as phosphorylation at the S330 site was markedly reduced in the respective knockouts (Fig. 7 and Fig. S4). Of note, β1 integrin is enriched in the outer Schwann cell membrane immediately overlying Cajal bands and β4 is present throughout the abaxonal membrane, including overlying the Cajal bands (Nodari et al., 2008; Court et al., 2011). β1 may activate PI 3-K by activating focal adhesion kinase and/or integrin-linked kinase (Reiske et al., 1999; Troussard et al., 2003), both of which play key roles in myelination (Grove et al., 2007; Pereira et al., 2009). However, the reduced phosphorylation of NDRG1 in the β1 knockout mice may be indirect—the result of aberrant myelination in these mice (Feltri et al., 2002), which would be expected to impair expression of both NDRG1 and β4 integrin.

We consider β4 the likely signaling receptor upstream of NDRG1. β4, which is obligately associated with α6, is dramatically up-regulated in Schwann cells at the onset of myelination in vivo and in vitro (Einheber et al., 1993; Feltri et al., 1994) with a time course and localization similar to that shown here for p-NDRG1. Further, phosphorylation of NDRG1, but not of S6rp, is markedly reduced in the β4 signaling mutant (Fig. 7). This truncated mutant lacks a cytoplasmic domain required for the activation of a number of downstream pathways, including PI 3-K (Guo et al., 2006; Giancotti, 2007). Unexpectedly, reduction of NDRG1 phosphorylation was more robust in the β4 signaling mutant than in the β4 knockout, as both the 3xThr and S330 sites were affected in the former. This may reflect compensation in β4 knockouts, including up-regulation of the β1 integrin subunit (Spinardi et al., 1995; Nodari et al., 2008), which does not occur in the knock-in signaling mutant. Alternatively, the signaling mutant may function in a dominant-negative manner.

Sgk1 is downstream of laminin-β4 integrin signaling

We have used NDRG1 to monitor signaling downstream of laminin and laminin receptors. Sgk1 has been thought to be the primary NDRG1 kinase; indeed, NDRG1 is widely used as a readout of Sgk1 activity (Pearce et al., 2011; Thomanetz et al., 2013). Consistent with this, NDRG1 phosphorylation is substantially reduced at both S330 and 3xThr in the Sgk1-null adult nerve (Fig. 8). But in the P10 nerve, Akt1 and Sgk1 both contribute to NDRG1 phosphorylation acting on the S330 and 3xThr sites, respectively (Fig. 8 and Fig. S5). These results indicate that Sgk1 is not the exclusive NDRG1 kinase and are

consistent with a recent report that altered Akt or Sgk expression results in compensatory changes in NDRG1 phosphorylation (Sommer et al., 2013). Taken together, these studies indicate that Akt1 and Sgk1 are expressed and phosphorylate NDRG1 in the developing peripheral nerve, whereas Sgk1 is the predominant NDRG1 kinase in the adult.

Two related questions concern the function of NDRG1 in myelination and the consequences of phosphorylation on its function. In addition to Schwann cells, NDRG1 is widely expressed by many types of cells. It has been extensively studied as a metastasis suppressor that promotes differentiation and antagonizes cell cycle progression (Melotte et al., 2010; Bae et al., 2013). However, the most important phenotype exhibited by NDRG1 nulls is a demyelinating neuropathy (Okuda et al., 2004; King et al., 2011), i.e., Charcot Marie Tooth 4D (Kalaydjieva et al., 2000). The requirement for NDRG1 in myelin maintenance and its localization to the Cajal bands raises the possibility these structures may also contribute to myelin maintenance. In the future, it will be of interest to determine whether loss of NDRG1 affects transport, signaling, and/or maintenance of the Cajal bands.

Our results suggest that NDRG1 phosphorylation may be dispensable for its function in myelination. In the Sgk1-null and β4 signaling mutant nerves, NDRG1 phosphorylation was markedly reduced (Figs. 7 and 8) without any clear effect on myelin stability at early ages and without an overt clinical phenotype. Analysis of myelin structure in the adult mutant mice will be useful to address this directly. However, even a small amount of functional NDRG1 significantly decreases the severity of demyelination displayed in the *stretcher* model (King et al., 2011). Thus, even if NDRG1 phosphorylation is necessary for its function, the residual p-NDRG1 in the Sgk1-null nerves may be sufficient for its role in myelin maintenance.

Spatial segregation of signaling

Our data indicate that the PI 3-K signaling pathways in the adaxonal and abaxonal compartments are functionally distinct and spatially segregated. There is a marked PI 3-K substrate preference in each compartment despite the potential for communication between them provided by the paranodes and incisures (Balice-Gordon et al., 1998). Thus, loss of Neuregulin1 and laminin in the co-cultures and in vivo results in an asymmetric reduction in mTOR activation and NDRG1 phosphorylation, respectively. Similarly, loss of β4 signaling reduces phosphorylation of NDRG1 but not of S6rp (Fig. 7 B).

This asymmetric phosphorylation is compartment specific, not ligand specific. In Schwann cells grown alone or under nonmyelinating co-cultures, which lack distinct cytoplasmic compartments, addition of either laminin or soluble Neuregulin1 results in phosphorylation of both NDRG1 and S6rp (Fig. S3). In contrast, after myelination, despite the broad expression of NDRG1, its phosphorylation is restricted to the abaxonal compartment and outer portions of the clefts (Fig. 5, A and B). These latter results indicate that signaling from integrins is confined to the abaxon, and to the Cajal bands in particular. Whether other key signaling pathways are also localized to specific compartments, as seems likely (Terada et al., 2013), will be of interest for further investigation.

Laminin-β4 integrin-Sgk1 signaling negatively regulates myelination

As laminin signals have long been considered to be promyelinating (Bunge et al., 1986), we were surprised that loss of β4 signaling and Sgk1 enhanced myelination at P10. This was most pronounced in the case of the Sgk1 mutants, which exhibit a dose-dependent increase in myelin thickness, more advanced segregation of large-caliber axons, and examples of multiple small axons myelinated en masse by single Schwann cells (Fig. 9). The β4 signaling mutant also exhibited evidence of hypermyelination, most evident in mid-sized fibers (Fig. 9 D and Fig. S5 A). Of note, some of the abnormalities in the developing Sgk1-null nerve partially phenocopy laminin and dystroglycan complex mutants. Although the most striking defects of the α2 and α4 laminin knockouts are a failure of radial sorting and of myelin initiation, these nerves also display examples of hypermyelinated fibers and polyaxonal myelination, respectively (Bradley and Jenkison, 1973; Wallquist et al., 2005). Hypermyelination of axons and polyaxonal myelination have also been observed in human dystrophic nerves (Di Muzio et al., 2003) and mice with conditional ablation of dystroglycan or periaxin (Gillespie et al., 2000; Saito et al., 2003). Thus, laminin and laminin-dependent pathways appear to have multiple functions during myelination—an initial, essential role in axon wrapping in which Rac1 signaling has been implicated (Nodari et al., 2007) and, based on these studies, a subsequent role as a negative regulator of myelination via Sgk1 activation.

The mechanism(s) responsible for hypermyelination in the Sgk1 nulls is not yet known but is of significant interest. Whether reduced phosphorylation of NDRG1 contributes, or acts in concert with, other as yet to be identified Sgk1 targets to mediate these effects are important questions for future study. Identification of these Sgk1 effectors may provide novel therapeutic targets to enhance myelin repair.

Materials and methods

Neuron, Schwann cell, and myelinating co-cultures

Primary and myelinating co-cultures were established as described previously (Maurel et al., 2007). In brief, dorsal root ganglia (DRG) were removed from E16 rats or E14 mice and dissociated for 45 min with 0.25% (vol/vol) trypsin (Life Technologies) or applied directly to pre-coated 12-mm coverslips (Karl Hecht GmbH) for explant cultures. Unless otherwise noted, coverslips were coated with collagen (Trevigen, Inc.). Cultures were maintained in Nunclon 4-well tissue culture plates (Thermo Fisher Scientific) at 37°C and 5% CO_2. Pure neuron cultures were obtained by cycling the cultures with C-media in the presence or absence of 10 µM fluorodeoxyuridine (Sigma-Aldrich) for 2 wk; C-media is based in MEM (Life Technologies) and contains 10% fetal calf serum (FCS; Life Technologies), 0.4% (wt/vol) glucose (Sigma-Aldrich), 50 µg/µL 2.5S NGF (AbD Serotec), and 2 mM L-glutamine (Life Technologies). Organotypic cultures were maintained in C-media for two feedings before the use of C+C media (i.e., C-media with 0.05 mg/ml ascorbate; Sigma-Aldrich) to induce myelination. Neuron cultures were seeded with purified, neonatal sciatic nerve Schwann cells (1.5×10^5 cells per coverslip; Brockes et al., 1979) to obtain a co-culture; such cultures were maintained in C-media for nonmyelinating or C+C for myelinating conditions. Schwann cell cultures were maintained in Schwann cell media (SC-media) that contained MEM, 10 µM L-glutamine, 10% FCS, 4 µM forskolin (LC Labs), and 5 ng/ml glial growth factor (R&D Systems). Neurons from neuregulin1 type III mice were obtained from E13.5 timed pregnancies, genotyped as described previously (Taveggia et al., 2005), and maintained as described above.

Immunofluorescence

Cultures were washed twice in phosphate-buffered saline (PBS), fixed in 4% paraformaldehyde (Electron Microscopy Sciences) in PBS for 15 min at room temperature (RT), and quenched in 75 mM NH_4Cl (Sigma-Aldrich) and 25 mM glycine (Sigma-Aldrich) in PBS for 5 min at RT and washed once in PBS. Fixed cultures were extracted with methanol (Thermo Fisher Scientific) for 10 min at −20°C, then washed three times with blocking solution, which contains 5% (wt/vol) bovine serum albumin (BSA; Sigma-Aldrich), 0.25% (vol/vol) Tween 20 (Sigma Aldrich), and 1% (vol/vol) normal donkey serum (Jackson ImmunoResearch Laboratories, Inc.). Primary antibodies were diluted in blocking solution, centrifuged for 10 min, then applied to the coverslips in a 30–50 µl volume overnight at 4°C. After incubation, cultures were washed three times with PBS (5 min each), and then secondary antibodies were applied in block for 90 min at RT. Cultures were then washed twice with PBS, a final time in distilled water, and mounted on slides with Citifluor (Citifluor Ltd.) with or without Hoechst (Life Technologies).

Teased sciatic nerve fibers were prepared from mouse or rat sciatic nerve as noted in the text and as reported previously (Maurel et al., 2007) with the following modifications: for p-Akt and Necl-4 immunofluorescence, each slide containing teased fibers was submerged in cold acetone for 15 min at −20°C, washed twice with PBS, and then marked with a liquid blocker pen (Daido Sangyo). The nerves were blocked for 1 h at RT in 2.5% (wt/vol) BSA, 1.5% (vol/vol) normal donkey serum, and 0.5% (vol/vol) Triton X-100 (Sigma-Aldrich). Application of primary and secondary antibodies and coverslipping was performed as described above. For α-DG immunofluorescence, nerve was fixed at RT for 45 min with 4% PFA in PBS. Nerves were permeabilized in methanol at RT for 5 min and blocked in 1% cold-water fish gelatin (Sigma-Aldrich) in PBS. Primary antibodies were applied in this blocking solution; secondary antibodies were applied in 5% (wt/vol) BSA, 1% (vol/vol) normal donkey serum, and 0.4% (vol/vol) Triton X-100 (Sigma-Aldrich).

Immunofluorescence image acquisition

Immunofluorescence images were obtained by laser-scanning confocal microscopy on a microscope (LSM 510; Carl Zeiss) using a 63× oil-immersion objective (Carl Zeiss) or a wide-field epifluorescence microscope (Eclipse Ti; Nikon) using 60× and 100× oil immersion objectives at RT. All images were taken of fixed cultures or sciatic nerve as noted in the text using Fluoromount-G mounting media (SouthernBiotech).

For confocal microscopy, a series of images taken in the vertical dimension using Z-stacking technology was compressed into a single image using the 3D projection tool of LSM Image Examiner software (version 4.0.0.421; Carl Zeiss). For wide-field imaging, we used the proprietary NIS-Elements AR 3.1 image acquisition software (Nikon) without deconvolution. In some cases, the brightness and contrast of immunofluorescence and immuno-EM images were adjusted in Photoshop CS5 (Adobe Systems); panels in each figure were processed equivalently.

Electron microscopy

Mice were perfused with 4% paraformaldehyde and 2.5% glutaraldehyde in 0.1 M phosphate buffer and 0.1 M D-sucrose at pH 7.4. Sciatic nerves were dissected and post-fixed in the same solution for 36 h, fixed in a solution of 1% osmium tetroxide in 0.1 M phosphate buffer, and progressively dehydrated in ethanol and propylene oxide. Finally, nerves were embedded in EMbed 812 (Epon 812 substitute) resin. All reagents used to prepare tissues for electron microscopy were purchased from Electron Microscopy Sciences.

Embedded nerves were cut into 70-nm ultrathin cross sections using a UCT microtome (Leica) and glass knife. Sections were placed on grids and stained with 3% uranyl acetate (aqueous) in 50% methanol and counterstained with Reynold's lead citrate. Sections were then visualized using an electron microscope (model CM12; Philips). The *g*-ratio was calculated by dividing the diameter of an axon (without the surrounding sheath) by the diameter of the same axon including the myelin sheath. Over 500 axons were calculated per mouse and two mice were analyzed per genotype. All measurements and ultrastructural abnormalities were recorded in a blinded fashion. G-ratios were calculated using NIS Elements AR imaging software (version 3.1; Nikon).

The processing of myelinating cultures for immunoelectron microscopy was performed as described previously with slight modifications (Einheber et al., 1993). Myelinating cultures grown on collagen-coated glass coverslips for 2 mo were rinsed in PBS containing a phosphatase inhibitor cocktail (Roche) and then fixed in 3.75% acrolein and 2% paraformaldehyde in 0.1 M sodium phosphate buffer, pH 7.4 (0.1 M PB) for 15 min at RT. After washing in 0.1 M PB the cultures were incubated in 0.5% sodium borohydride in 0.1 M PB for 30 min and then rinsed again in 0.1 M PB. The cultures were then dislodged from the coverslips with forceps and transferred to microfuge tubes containing 0.1 M PB. The samples were spun for 15 min in a microfuge to pellet the cultures and then embedded in LR White (The London Resin Co., Ltd.). To prepare samples for embedding, they were dehydrated by two 10-min incubations in 50, 60, 70, and 80% ethanol. The pellets were then incubated in two 1-h changes of a 1:1 mixture of 80% ethanol and LR White, four 30-min incubations with pure LR White, and an overnight incubation at 4°C in pure LR White. The next day the pellets were placed in gelatin capsules filled with fresh LR White and incubated in a 50°C oven for 2 d to polymerize the resin.

Ultrathin sections (70 nm) were placed on 400-mesh nickel grids. For post-embedding labeling the grids were subjected to five 2-min washes in PBSg (PBS containing 0.01 M glycine) and blocked for 10 min in PBSg containing 1% gelatin. After five 1-min washes in PBSg the grids were floated, section down, on 20-µl drops of primary antibodies diluted in PBSg/0.5% BSA or of diluent alone for controls without primary antibody in a moist chamber at 37°C for 3 h. The grids were then washed six times, 2 min each in PBSg, and incubated on 20-µl drops of 10-nm gold–conjugated goat anti–rabbit IgG (Electron Microscopy Sciences) in a moist chamber at RT for 45 min. Unbound secondary antibody was removed by six 2-min washes in PBSg and four 1-min washes in PBS. The grids were post-fixed in 2% glutaraldehyde/PBS for 15 min. After washing in PBS and then water, the grids were counterstained with uranyl acetate and lead citrate, washed, air dried, and analyzed on an electron microscope (model CM10; Philips).

Quantification was performed in a blind fashion by recording the number of immunogold particles in the adaxon, abaxon, and compact myelin and dividing by the number of total particles. From these values, we subtracted the ratios we obtained for each compartment in the "no primary" control as a background correction. G-ratios were measured blindly using the proprietary NIS-Elements AR 3.1 image acquisition software (Nikon).

Western blotting

Cultures were lysed with PBS containing 1% SDS, 95 mM NaCl, and 10 mM EDTA supplemented with protease and phosphatase inhibitors (Roche). Neonatal sciatic nerve lysates were prepared by flash-freezing with nitrogen, grinding the frozen tissue in the tube with a small pestle in a 75-µl volume, and sonicating briefly. Adult sciatic nerve was also flash-frozen in nitrogen and macerated in a conventional ceramic mortar and pestle before sonication. All lysates were heated for 3–5 min at 95°C and centrifuged before protein quantification by the BCA method (Thermo Fisher Scientific). Lysates (10–60 µg) were boiled in sample buffer (50 mM Tris-Cl, pH 6.8, 5% vol/vol β-mercaptoethanol, 2% [wt/vol] sodium dodecyl sulfate, 0.1% [wt/vol] bromophenol blue, and 10% [vol/vol] glycerol) before loading into a freshly cast polyacrylamide reducing gel and run with an infrared pre-stained ladder (LI-COR Biosciences). Gels were transferred to nitrocellulose membrane and blocked (5% nonfat dry milk in Tris-buffered saline) before primary antibody incubation overnight at 4°C (in 5% BSA in Tris-buffered saline and Tween 20). After three washing steps in Tris-buffered saline and Tween 20 (TBST), infrared-compatible secondary antibodies were applied for 90 min in 5% nonfat dry milk in TBST. After a final three washing steps in TBST, membranes were imaged and quantified using an Odyssey machine (LI-COR Biosciences).

Antibodies

Primary rabbit antibodies included: monoclonal and polyclonal Akt phosphosubstrate antibody (1:1,000 for blotting, 1:400 for staining; #9611 and #9614; Cell Signaling Technology); MBP (1:50 for immuno-EM; #AB980; EMD Millipore); NDRG1 p-Ser330 (1:350 for immunofluorescence and immuno-EM, 1:500 for blotting; #3506; Cell Signaling Technology); NDRG1 p-3xThr (1:350 for co-culture immunofluorescence, 1:2,500 for sciatic nerve immunofluorescence, 1:750 for blotting; #5482; Cell Signaling Technology); total NDRG1 (1:1,000 for co-culture immunofluorescence, 1:3,500 for sciatic nerve immunofluorescence, 1:3,000 for blotting; a gift of U. Suter, ETH Zurich, Zurich, Switzerland); p-Akt Thr308 and Ser473 (1:75 for immunofluorescence, 1:500 for blotting; #2965 and #9271; Cell Signaling Technology); pan-Akt (1:1,250 for blotting; #9272; Cell Signaling Technology); Redd1 (1:100 blotting; Abcam); PTEN (1:750 blotting; #9559; Cell Signaling Technology); p-S6rp Ser235/6 (1:150 staining, 1:750 blotting, #4856; Cell Signaling Technology); total S6rp (1:1,200 blotting; #2217; Cell Signaling Technology); and MAG-ECD (1:100 for immuno-EM) was generated by our laboratory as described previously (Pedraza et al., 1990). Mouse monoclonal antibodies included: γ1-laminin (1:25 for immunofluorescence; clone D18; DSHB, Iowa City, Iowa); anti–β-actin clone AC15 (1:5,000 for blotting; #A-5441; Sigma-Aldrich);

α-dystroglycan antibody clone IIH6 (1:400 for staining; a gift of K. Campbell, University of Iowa, Iowa City, IA; Ervasti and Campbell, 1993); and Dlg1/Sap97 clone K64/15 (1:250 for blotting; Neuromab, University of California, Davis, Davis, CA). Guinea pig antibodies included: Caspr1 (1:3,000 for immunofluorescence; a gift of M. Bhat, University of Texas Health Science Center, San Antonio, TX); Necl-4 generated in our laboratory and used for staining as described previously (Maurel et al., 2007); Oct6/POU3F1 (1:16,000 for immunofluorescence; a gift from J. Dasen, NYU School of Medicine, New York, NY). Other antibodies were chicken anti-MBP (1:50 for immunofluorescence and 1:750 for blotting; #AB9348; EMD Millipore), chicken anti-P0 (1:50 for immunofluorescence and 1:1,000 for blotting; #AB9352; EMD Millipore); sheep anti-Mupp1 (1:100 for immunofluorescence; from O. Peles, Weizmann Institute, Rehovot, Israel).

Secondary antibodies used for immunofluorescence were from Jackson ImmunoResearch Laboratories, Inc., and raised in donkey and conjugated to either rhodamine, Alexa Fluor 488, Cy5, Dylight649, or AMCA. Secondary antibodies for Western blotting were from LI-COR Biosciences, raised in goat, and conjugated to IRDye800 or IRDye680 for dual-color infrared detection.

Schwann cell induction and inhibition

Pure Schwann cells and Schwann cell–neuron co-cultures maintained in nonmyelinating media for 10–14 d were briefly washed three times in warmed starvation media (MEM and 10 µM L-glutamine). Cultures were incubated in starvation media for 5–6 h in the presence or absence of 20 µM LY294002 (LC Labs). Aliquots of 10 µg/ml natural mouse laminin (Life Technologies) or 1 mg/ml Matrigel (BD) were diluted freshly in the presence or absence of 20 µM LY294002 in the same media. At the end of the incubation, pre-warmed preparations of diluted natural mouse laminin or Matrigel were applied to the cultures for 30 min. Cells were then placed on ice and rinsed with pre-chilled PBS before lysis.

Non-myelinating co-cultures of Schwann cells and sensory neurons were maintained in serum-containing media for 48 h before an 18-h application of 20 µM LY294004 (LC Labs), 25 nM rapamycin (LC Labs), or 40 µM PF4708671 (Sigma-Aldrich) in defined, serum-free media.

Reverse-transcription PCR

Isolation of mRNA from pure cultures of rat sensory neurons or Schwann cells was performed with TRIzol reagent (Life Technologies) according to the manufacturer's instructions. The mRNA was resuspended in Ambion RNA storage solution (Life Technologies) and quantified using a spectrophotometer (model DU-800; Beckman Coulter). 1 µg of mRNA was used to make 20 µl of cDNA using an RNase Easy kit (QIAGEN). For each PCR reaction performed with the Fermentas DreamTaq master mix (Thermo Fisher Scientific), 1 µl of cDNA was used. The PCR program for all primers involved 30 cycles of denaturation at 95°C, annealing at 60°C, and extension at 72°C followed by an additional final extension step before holding at 4°C. Primers were designed using the NCBI Blast tool to confirm specificity and standardize product size to ∼100 bp. The GAPDH primer pair spans an intron–exon junction. The primer sequences are listed in the 5′ to 3′ direction as follows: GAPDH fwd, ACAAGATGGTGAAGGTCGGTGTGA; GAPDH rev, AGCTTCCCATTCTCAGCCTTGACT; Sgk1 fwd, GCTCCCAGGATGGTTCCGAAGGA; Sgk1 rev, TCCGGAAAGCTTCCGCGTCA; Sgk2 fwd, AGTCAGGCGAGTGGGTGACAGG; Sgk2 rev, TGGAAACCCCCAGGTTCCAGC; and Sgk3 fwd, TCGCTATTTCTGATACCACCACAACC; Sgk3 rev, AGGCTCACTCCTGGTCTCAAGTTCA.

Mouse models

All of the mouse models used in this project have been described previously. The α2-laminin knockout was generated by knocking a pMC1neo polyA+ cassette (Agilent Technologies) into an exon (aa 128–209) as described previously (Nakagawa et al., 2001). The β1 integrin conditional allele was generated by targeting two *loxP* sites to both sides of the first coding exon of the gene (Graus-Porta et al., 2001; Feltri et al., 2002). The β4 integrin conditional allele (Nodari et al., 2008) was generated using the mβ4intλc targeting vector, which contains the first 7 introns and exons of β4 genomic DNA and the necessary *loxP* sites (Dowling et al., 1996). The dystroglycan conditional allele was generated by inserting a floxed NEO cassette into the exon 2 locus (Moore et al., 2002). The P0-CRE line was generated by cloning in recombinant CRE downstream of the full-length 6-kb promoter of the mouse P0 gene (Feltri et al., 1999). Two Sgk1-null lines in the same C57/Sv129 mixed background were used in this study. The first was generated by cloning a *loxP* site into intron 1 and two others in intron 6 flanking a NEO cassette (which was flanked by FRT sites) and mated with the global Cre-deleter line BALB/c-Tg(CMV-cre)1Gcn/J from The Jackson Laboratory (Fejes-Tóth et al., 2008). The other Sgk1-null line was generated using a similar approach in which a *loxP* site was introduced into intron 3 and two others flanking a NEO casette in intron 11; the resulting homologously recombined ES cell clones were then transiently transfected with Cre recombinase (Wulff et al., 2002). The Sgk3-null animal was generated by replacing parts of exons 10 and 11 as well as the intron between them with an in-frame STOP codon (McCormick et al., 2004). The β4 integrin–signaling mutant was generated by replacing the signaling moiety of the cytoplasmic domain of β4 C-terminal to Thr1355 with a stop codon, a SV40 polyadenylation signal, and a NEO cassette (Nikolopoulos et al., 2004). The *stretcher* mouse is a spontaneous deletion of exons 10–14 of the *Ndrg1* gene (King et al., 2011). The Neuregulin1 type III CRD-null mouse was generated by homologous recombination of a nonsense mutation and an antisense NEO cassette into the cysteine-rich domain region of the *Neuregulin1* gene (Wolpowitz et al., 2000). All three Akt isoform-specific mice were obtained from The Jackson Laboratory.

Statistical methods

All one-way ANOVA and two-tailed Student's *t* tests performed were computed using Excel 2007 (Microsoft) or Prism (GraphPad Software).

Online supplemental material

Fig. S1 demonstrates the subcellular localization of NDRG1 and phospho-substrates. Fig. S1 A shows that total and phospho-specific NDRG1 antibodies stained wild type but not *stretcher* co-cultures, indicating they are specific. Fig. S1 B shows that staining of *stretcher* cultures with the p-Sub–staining antibody was reduced, notably in the abaxon, but was not abolished. Fig. S1 C demonstrates that p-Akt localizes to the paranodes, identified by expression of Caspr, as myelin sheaths mature; p-Akt is similarly localized to the paranodes of neonatal sciatic nerves. Fig. S2 A shows ultrastructural localization of p-NDRG1, myelin-associated glycoprotein, and MBP by immunoelectron microscopy of myelinating co-cultures, quantified in Fig. S2 B; these results support an abaxonal localization of p-NDRG1 (S330). Fig. S2 C demonstrates that S6rp phosphorylation is dependent on Neuregulin1 type III expression in the co-cultures. Fig. S3 shows that adding Matrigel to pure Schwann cell cultures does not increase phosphorylation of NDRG1 (A), whereas adding Matrigel or laminin up-regulates phosphorylation of NDRG1 when Schwann cells are co-cultured with neurons (B), suggesting the laminin receptor is expressed in an axon-dependent manner; phosphorylation is blocked by the LY inhibitor. Fig. S3 C shows that soluble Neuregulin1 type III also increases NDRG1 phosphorylation in nonmyelinating cultures, which lack distinct cytoplasmic compartments. Fig. S4 A demonstrates how laminin receptors, particularly β4 integrin, are necessary for phosphorylation of NDRG1 but not S6rp. Fig. S4, C and D show that kinases that phosphorylated NDRG1 include Akt1 and Sgk1 at P10 and Sgk1 and Sgk3 in the adult nerve. Fig. S5 A demonstrates that loss of β4 integrin signaling causes modest hypermyelination. Fig. S5 B shows that hypermyelination in the Sgk1 nulls is unlikely to be the result of known negative regulators of myelination such as DLG1 and REDD1; thus, whereas REDD1 levels were modestly reduced, mTOR activity (indicated by p-S6rp levels), its negatively regulated effector, was not consistently increased. Online supplemental material is available at http://www.jcb.org/cgi/content/full/jcb.201307057/DC1.

We thank U. Suter and S. Scherer for the total NDRG1 antibody, M. Bhat for Caspr1 antibody, E. Peles for Mupp1 antibody, K. Campbell for the dystroglycan antibody, and A. Bolino for the Redd1 antibody. We also acknowledge A. Liang, C. Petzold, and K. Dancel of the NYULMC OCS Microscopy Core and T. Milner of Weill Cornell Medical College for their assistance with TEM work. We also thank A. Pepe-Caprio (Memorial Sloan-Kettering Cancer Center) for her assistance with the β4-signaling mutant line.

This work was supported by National Institutes of Health grants NS26001 (J.L. Salzer), DK41481 (A.N. Fejes-Toth), DK58898 (G. Fejes-Toth), and R01 CA129023 (F. Giancotti); as well as Telethon Italia GPP1007A (M.L. Feltri), Association Francaise contre les Myopathies, and the National Health and Medical Research Council of Australia (L. Kalaydjieva).

The authors declare no competing financial interests.

Submitted: 9 July 2013
Accepted: 18 February 2014

References

Alessi, D.R., F.B. Caudwell, M. Andjelkovic, B.A. Hemmings, and P. Cohen. 1996. Molecular basis for the substrate specificity of protein kinase B; comparison with MAPKAP kinase-1 and p70 S6 kinase. *FEBS Lett.* 399:333–338. http://dx.doi.org/10.1016/S0014-5793(96)01370-1

Alessi, D.R., M. Deak, A. Casamayor, F.B. Caudwell, N. Morrice, D.G. Norman, P. Gaffney, C.B. Reese, C.N. MacDougall, D. Harbison, et al. 1997a. 3-Phosphoinositide-dependent protein kinase-1 (PDK1): structural and functional homology with the *Drosophila* DSTPK61 kinase. *Curr. Biol.* 7:776–789. http://dx.doi.org/10.1016/S0960-9822(06)00336-8

Alessi, D.R., S.R. James, C.P. Downes, A.B. Holmes, P.R. Gaffney, C.B. Reese, and P. Cohen. 1997b. Characterization of a 3-phosphoinositide-dependent protein kinase which phosphorylates and activates protein kinase Balpha. *Curr. Biol.* 7:261–269. http://dx.doi.org/10.1016/S0960-9822(06)00122-9

Atanasoski, S., S.S. Scherer, E. Sirkowski, D. Leone, A.N. Garratt, C. Birchmeier, and U. Suter. 2006. ErbB2 signaling in Schwann cells is mostly dispensable for maintenance of myelinated peripheral nerves and proliferation of adult Schwann cells after injury. *J. Neurosci.* 26:2124–2131. http://dx.doi.org/10.1523/JNEUROSCI.4594-05.2006

Bae, D.H., P.J. Jansson, M.L. Huang, Z. Kovacevic, D. Kalinowski, C.S. Lee, S. Sahni, and D.R. Richardson. 2013. The role of NDRG1 in the pathology and potential treatment of human cancers. *J. Clin. Pathol.* 66:911–917. http://dx.doi.org/10.1136/jclinpath-2013-201692

Balice-Gordon, R.J., L.J. Bone, and S.S. Scherer. 1998. Functional gap junctions in the Schwann cell myelin sheath. *J. Cell Biol.* 142:1095–1104. http://dx.doi.org/10.1083/jcb.142.4.1095

Berger, P., E.E. Sirkowski, S.S. Scherer, and U. Suter. 2004. Expression analysis of the N-Myc downstream-regulated gene 1 indicates that myelinating Schwann cells are the primary disease target in hereditary motor and sensory neuropathy-Lom. *Neurobiol. Dis.* 17:290–299. http://dx.doi.org/10.1016/j.nbd.2004.07.014

Bermingham, J.R. Jr., S.S. Scherer, S. O'Connell, E. Arroyo, K.A. Kalla, F.L. Powell, and M.G. Rosenfeld. 1996. Tst-1/Oct-6/SCIP regulates a unique step in peripheral myelination and is required for normal respiration. *Genes Dev.* 10:1751–1762. http://dx.doi.org/10.1101/gad.10.14.1751

Berti, C., L. Bartesaghi, M. Ghidinelli, D. Zambroni, G. Figlia, Z.L. Chen, A. Quattrini, L. Wrabetz, and M.L. Feltri. 2011. Non-redundant function of dystroglycan and β1 integrins in radial sorting of axons. *Development*. 138:4025–4037. http://dx.doi.org/10.1242/dev.065490

Bradley, W.G., and M. Jenkison. 1973. Abnormalities of peripheral nerves in murine muscular dystrophy. *J. Neurol. Sci.* 18:227–247. http://dx.doi.org/10.1016/0022-510X(73)90009-9

Brockes, J.P., K.L. Fields, and M.C. Raff. 1979. Studies on cultured rat Schwann cells. I. Establishment of purified populations from cultures of peripheral nerve. *Brain Res.* 165:105–118. http://dx.doi.org/10.1016/0006-8993(79)90048-9

Bunge, R.P., M.B. Bunge, and C.F. Eldridge. 1986. Linkage between axonal ensheathment and basal lamina production by Schwann cells. *Annu. Rev. Neurosci.* 9:305–328. http://dx.doi.org/10.1146/annurev.ne.09.030186.001513

Bunge, R.P., M.B. Bunge, and M. Bates. 1989. Movements of the Schwann cell nucleus implicate progression of the inner (axon-related) Schwann cell process during myelination. *J. Cell Biol.* 109:273–284. http://dx.doi.org/10.1083/jcb.109.1.273

Burchfield, J.G., A.J. Lennard, S. Narasimhan, W.E. Hughes, V.C. Wasinger, G.L. Corthals, T. Okuda, H. Kondoh, T.J. Biden, and C. Schmitz-Peiffer. 2004. Akt mediates insulin-stimulated phosphorylation of Ndrg2: evidence for cross-talk with protein kinase C theta. *J. Biol. Chem.* 279:18623–18632. http://dx.doi.org/10.1074/jbc.M401504200

Canoll, P.D., J.M. Musacchio, R. Hardy, R. Reynolds, M.A. Marchionni, and J.L. Salzer. 1996. GGF/neuregulin is a neuronal signal that promotes the proliferation and survival and inhibits the differentiation of oligodendrocyte progenitors. *Neuron*. 17:229–243. http://dx.doi.org/10.1016/S0896-6273(00)80155-5

Cantley, L.C. 2002. The phosphoinositide 3-kinase pathway. *Science*. 296:1655–1657. http://dx.doi.org/10.1126/science.296.5573.1655

Cotter, L., M. Ozçelik, C. Jacob, J.A. Pereira, V. Locher, R. Baumann, J.B. Relvas, U. Suter, and N. Tricaud. 2010. Dlg1-PTEN interaction regulates myelin thickness to prevent damaging peripheral nerve overmyelination. *Science*. 328:1415–1418. http://dx.doi.org/10.1126/science.1187735

Court, F.A., D.L. Sherman, T. Pratt, E.M. Garry, R.R. Ribchester, D.F. Cottrell, S.M. Fleetwood-Walker, and P.J. Brophy. 2004. Restricted growth of Schwann cells lacking Cajal bands slows conduction in myelinated nerves. *Nature*. 431:191–195. http://dx.doi.org/10.1038/nature02841

Court, F.A., D. Zambroni, E. Pavoni, C. Colombelli, C. Baragli, G. Figlia, L. Sorokin, W. Ching, J.L. Salzer, L. Wrabetz, and M.L. Feltri. 2011. MMP2-9 cleavage of dystroglycan alters the size and molecular composition of Schwann cell domains. *J. Neurosci.* 31:12208–12217. http://dx.doi.org/10.1523/JNEUROSCI.0141-11.2011

Di Muzio, A., M.V. De Angelis, P. Di Fulvio, A. Ratti, A. Pizzuti, L. Stuppia, D. Gambi, and A. Uncini. 2003. Dysmyelinating sensory-motor neuropathy in merosin-deficient congenital muscular dystrophy. *Muscle Nerve*. 27:500–506. http://dx.doi.org/10.1002/mus.10326

Dowling, J., Q.C. Yu, and E. Fuchs. 1996. Beta4 integrin is required for hemidesmosome formation, cell adhesion and cell survival. *J. Cell Biol.* 134:559–572. http://dx.doi.org/10.1083/jcb.134.2.559

Einheber, S., T.A. Milner, F. Giancotti, and J.L. Salzer. 1993. Axonal regulation of Schwann cell integrin expression suggests a role for alpha 6 beta 4 in myelination. *J. Cell Biol.* 123:1223–1236. http://dx.doi.org/10.1083/jcb.123.5.1223

Eldridge, C.F., M.B. Bunge, R.P. Bunge, and P.M. Wood. 1987. Differentiation of axon-related Schwann cells in vitro. I. Ascorbic acid regulates basal lamina assembly and myelin formation. *J. Cell Biol.* 105:1023–1034. http://dx.doi.org/10.1083/jcb.105.2.1023

Ervasti, J.M., and K.P. Campbell. 1993. A role for the dystrophin-glycoprotein complex as a transmembrane linker between laminin and actin. *J. Cell Biol.* 122:809–823. http://dx.doi.org/10.1083/jcb.122.4.809

Fannon, A.M., D.L. Sherman, G. Ilyina-Gragerova, P.J. Brophy, V.L. Friedrich Jr., and D.R. Colman. 1995. Novel E-cadherin-mediated adhesion in peripheral nerve: Schwann cell architecture is stabilized by autotypic adherens junctions. *J. Cell Biol.* 129:189–202. http://dx.doi.org/10.1083/jcb.129.1.189

Fejes-Tóth, G., G. Frindt, A. Náray-Fejes-Tóth, and L.G. Palmer. 2008. Epithelial Na+ channel activation and processing in mice lacking SGK1. *Am. J. Physiol. Renal Physiol.* 294:F1298–F1305. http://dx.doi.org/10.1152/ajprenal.00579.2007

Feltri, M.L., and L. Wrabetz. 2005. Laminins and their receptors in Schwann cells and hereditary neuropathies. *J. Peripher. Nerv. Syst.* 10:128–143. http://dx.doi.org/10.1111/j.1085-9489.2005.0010204.x

Feltri, M.L., S.S. Scherer, R. Nemni, J. Kamholz, H. Vogelbacker, M.O. Scott, N. Canal, V. Quaranta, and L. Wrabetz. 1994. Beta 4 integrin expression in myelinating Schwann cells is polarized, developmentally regulated and axonally dependent. *Development*. 120:1287–1301.

Feltri, M.L., M. D'Antonio, S. Previtali, M. Fasolini, A. Messing, and L. Wrabetz. 1999. P0-Cre transgenic mice for inactivation of adhesion molecules in Schwann cells. *Ann. N. Y. Acad. Sci.* 883(1 CHARCOT-MARIE):116–123. http://dx.doi.org/10.1111/j.1749-6632.1999.tb08574.x

Feltri, M.L., D. Graus Porta, S.C. Previtali, A. Nodari, B. Migliavacca, A. Cassetti, A. Littlewood-Evans, L.F. Reichardt, A. Messing, A. Quattrini, et al. 2002. Conditional disruption of beta 1 integrin in Schwann cells impedes interactions with axons. *J. Cell Biol.* 156:199–209. http://dx.doi.org/10.1083/jcb.200109021

Fricker, F.R., N. Zhu, C. Tsantoulas, B. Abrahamsen, M.A. Nassar, M. Thakur, A.N. Garratt, C. Birchmeier, S.B. McMahon, J.N. Wood, and D.L. Bennett. 2009. Sensory axon-derived neuregulin-1 is required for axoglial signaling and normal sensory function but not for long-term axon maintenance. *J. Neurosci.* 29:7667–7678. http://dx.doi.org/10.1523/JNEUROSCI.6053-08.2009

Giancotti, F.G. 2007. Targeting integrin beta4 for cancer and anti-angiogenic therapy. *Trends Pharmacol. Sci.* 28:506–511. http://dx.doi.org/10.1016/j.tips.2007.08.004

Gillespie, C.S., D.L. Sherman, S.M. Fleetwood-Walker, D.F. Cottrell, S. Tait, E.M. Garry, V.C. Wallace, J. Ure, I.R. Griffiths, A. Smith, and P.J. Brophy. 2000. Peripheral demyelination and neuropathic pain behavior in periaxin-deficient mice. *Neuron*. 26:523–531. http://dx.doi.org/10.1016/S0896-6273(00)81184-8

Glenn, T.D., and W.S. Talbot. 2013. Signals regulating myelination in peripheral nerves and the Schwann cell response to injury. *Curr. Opin. Neurobiol.* 23:1041–1048. http://dx.doi.org/10.1016/j.conb.2013.06.010

Goebbels, S., J.H. Oltrogge, R. Kemper, I. Heilmann, I. Bormuth, S. Wolfer, S.P. Wichert, W. Möbius, X. Liu, C. Lappe-Siefke, et al. 2010. Elevated phosphatidylinositol 3,4,5-trisphosphate in glia triggers cell-autonomous membrane wrapping and myelination. *J. Neurosci.* 30:8953–8964. http://dx.doi.org/10.1523/JNEUROSCI.0219-10.2010

Gould, R.M., and G. Mattingly. 1990. Regional localization of RNA and protein metabolism in Schwann cells in vivo. *J. Neurocytol.* 19:285–301. http://dx.doi.org/10.1007/BF01188399

Graus-Porta, D., S. Blaess, M. Senften, A. Littlewood-Evans, C. Damsky, Z. Huang, P. Orban, R. Klein, J.C. Schittny, and U. Müller. 2001. β1-class integrins regulate the development of laminae and folia in the cerebral and cerebellar cortex. *Neuron*. 31:367–379. http://dx.doi.org/10.1016/S0896-6273(01)00374-9

Griffin, J.W., and W.J. Thompson. 2008. Biology and pathology of nonmyelinating Schwann cells. *Glia*. 56:1518–1531. http://dx.doi.org/10.1002/glia.20778

Grove, M., N.H. Komiyama, K.A. Nave, S.G. Grant, D.L. Sherman, and P.J. Brophy. 2007. FAK is required for axonal sorting by Schwann cells. *J. Cell Biol.* 176:277–282. http://dx.doi.org/10.1083/jcb.200609021

Guo, W., Y. Pylayeva, A. Pepe, T. Yoshioka, W.J. Muller, G. Inghirami, and F.G. Giancotti. 2006. Beta 4 integrin amplifies ErbB2 signaling to promote mammary tumorigenesis. *Cell*. 126:489–502. http://dx.doi.org/10.1016/j.cell.2006.05.047

Jaegle, M., M. Ghazvini, W. Mandemakers, M. Piirsoo, S. Driegen, F. Levavasseur, S. Raghoenath, F. Grosveld, and D. Meijer. 2003. The POU proteins Brn-2 and Oct-6 share important functions in Schwann cell development. *Genes Dev.* 17:1380–1391. http://dx.doi.org/10.1101/gad.258203

Kalaydjieva, L., D. Gresham, R. Gooding, L. Heather, F. Baas, R. de Jonge, K. Blechschmidt, D. Angelicheva, D. Chandler, P. Worsley, et al. 2000. N-myc downstream-regulated gene 1 is mutated in hereditary motor and sensory neuropathy-Lom. *Am. J. Hum. Genet.* 67:47–58. http://dx.doi.org/10.1086/302978

Kamimura, Y., Y. Xiong, P.A. Iglesias, O. Hoeller, P. Bolourani, and P.N. Devreotes. 2008. PIP3-independent activation of TorC2 and PKB at the cell's leading edge mediates chemotaxis. *Curr. Biol.* 18:1034–1043. http://dx.doi.org/10.1016/j.cub.2008.06.068

Kane, S., H. Sano, S.C. Liu, J.M. Asara, W.S. Lane, C.C. Garner, and G.E. Lienhard. 2002. A method to identify serine kinase substrates. Akt phosphorylates a novel adipocyte protein with a Rab GTPase-activating protein (GAP) domain. *J. Biol. Chem.* 277:22115–22118. http://dx.doi.org/10.1074/jbc.C200198200

Kao, S.C., H. Wu, J. Xie, C.P. Chang, J.A. Ranish, I.A. Graef, and G.R. Crabtree. 2009. Calcineurin/NFAT signaling is required for neuregulin-regulated Schwann cell differentiation. *Science*. 323:651–654. http://dx.doi.org/10.1126/science.1166562

King, R.H., D. Chandler, S. Lopaticki, D. Huang, J. Blake, J.R. Muddle, T. Kilpatrick, M. Nourallah, T. Miyata, T. Okuda, et al. 2011. Ndrg1 in development and maintenance of the myelin sheath. *Neurobiol. Dis.* 42:368–380. http://dx.doi.org/10.1016/j.nbd.2011.01.030

Kobayashi, T., M. Deak, N. Morrice, and P. Cohen. 1999. Characterization of the structure and regulation of two novel isoforms of serum- and glucocorticoid-induced protein kinase. *Biochem. J.* 344:189–197. http://dx.doi.org/10.1042/0264-6021:3440189

Laplante, M., and D.M. Sabatini. 2013. Regulation of mTORC1 and its impact on gene expression at a glance. *J. Cell Sci.* 126:1713–1719. http://dx.doi.org/10.1242/jcs.125773

Maehama, T., and J.E. Dixon. 1998. The tumor suppressor, PTEN/MMAC1, dephosphorylates the lipid second messenger, phosphatidylinositol 3,4,5-trisphosphate. *J. Biol. Chem.* 273:13375–13378. http://dx.doi.org/10.1074/jbc.273.22.13375

Magnuson, B., B. Ekim, and D.C. Fingar. 2012. Regulation and function of ribosomal protein S6 kinase (S6K) within mTOR signalling networks. *Biochem. J.* 441:1–21. http://dx.doi.org/10.1042/BJ20110892

Maurel, P., and J.L. Salzer. 2000. Axonal regulation of Schwann cell proliferation and survival and the initial events of myelination requires PI 3-kinase activity. *J. Neurosci.* 20:4635–4645.

Maurel, P., S. Einheber, J. Galinska, P. Thaker, I. Lam, M.B. Rubin, S.S. Scherer, Y. Murakami, D.H. Gutmann, and J.L. Salzer. 2007. Nectin-like proteins mediate axon Schwann cell interactions along the internode and are essential for myelination. *J. Cell Biol.* 178:861–874. http://dx.doi.org/10.1083/jcb.200705132

McCormick, J.A., Y. Feng, K. Dawson, M.J. Behne, B. Yu, J. Wang, A.W. Wyatt, G. Henke, F. Grahammer, T.M. Mauro, et al. 2004. Targeted disruption of the protein kinase SGK3/CISK impairs postnatal hair follicle development. *Mol. Biol. Cell*. 15:4278–4288. http://dx.doi.org/10.1091/mbc.E04-01-0027

Melotte, V., X. Qu, M. Ongenaert, W. van Criekinge, A.P. de Bruïne, H.S. Baldwin, and M. van Engeland. 2010. The N-myc downstream regulated gene (NDRG) family: diverse functions, multiple applications. *FASEB J.* 24:4153–4166. http://dx.doi.org/10.1096/fj.09-151464

Michailov, G.V., M.W. Sereda, B.G. Brinkmann, T.M. Fischer, B. Haug, C. Birchmeier, L. Role, C. Lai, M.H. Schwab, and K.A. Nave. 2004. Axonal neuregulin-1 regulates myelin sheath thickness. *Science*. 304:700–703. http://dx.doi.org/10.1126/science.1095862

Moore, S.A., F. Saito, J. Chen, D.E. Michele, M.D. Henry, A. Messing, R.D. Cohn, S.E. Ross-Barta, S. Westra, R.A. Williamson, et al. 2002. Deletion of brain dystroglycan recapitulates aspects of congenital muscular dystrophy. *Nature*. 418:422–425. http://dx.doi.org/10.1038/nature00838

Mora, A., D. Komander, D.M. van Aalten, and D.R. Alessi. 2004. PDK1, the master regulator of AGC kinase signal transduction. *Semin. Cell Dev. Biol.* 15:161–170. http://dx.doi.org/10.1016/j.semcdb.2003.12.022

Murray, J.T., D.G. Campbell, N. Morrice, G.C. Auld, N. Shpiro, R. Marquez, M. Peggie, J. Bain, G.B. Bloomberg, F. Grahammer, et al. 2004. Exploitation of KESTREL to identify NDRG family members as physiological substrates for SGK1 and GSK3. *Biochem. J.* 384:477–488. http://dx.doi.org/10.1042/BJ20041057

Nakagawa, M., Y. Miyagoe-Suzuki, K. Ikezoe, Y. Miyata, I. Nonaka, K. Harii, and S. Takeda. 2001. Schwann cell myelination occurred without basal lamina formation in laminin alpha2 chain-null mutant (dy3K/dy3K) mice. *Glia*. 35:101–110. http://dx.doi.org/10.1002/glia.1075

Nave, K.A., and J.L. Salzer. 2006. Axonal regulation of myelination by neuregulin 1. *Curr. Opin. Neurobiol.* 16:492–500. http://dx.doi.org/10.1016/j.conb.2006.08.008

Newbern, J.M., X. Li, S.E. Shoemaker, J. Zhou, J. Zhong, Y. Wu, D. Bonder, S. Hollenback, G. Coppola, D.H. Geschwind, et al. 2011. Specific functions for ERK/MAPK signaling during PNS development. *Neuron*. 69:91–105. http://dx.doi.org/10.1016/j.neuron.2010.12.003

Nikolopoulos, S.N., P. Blaikie, T. Yoshioka, W. Guo, and F.G. Giancotti. 2004. Integrin beta4 signaling promotes tumor angiogenesis. *Cancer Cell*. 6:471–483. http://dx.doi.org/10.1016/j.ccr.2004.09.029

Nodari, A., D. Zambroni, A. Quattrini, F.A. Court, A. D'Urso, A. Recchia, V.L. Tybulewicz, L. Wrabetz, and M.L. Feltri. 2007. Beta1 integrin activates Rac1 in Schwann cells to generate radial lamellae during axonal sorting and myelination. *J. Cell Biol.* 177:1063–1075. http://dx.doi.org/10.1083/jcb.200610014

Nodari, A., S.C. Previtali, G. Dati, S. Occhi, F.A. Court, C. Colombelli, D. Zambroni, G. Dina, U. Del Carro, K.P. Campbell, et al. 2008. Alpha6beta4 integrin and dystroglycan cooperate to stabilize the myelin sheath. *J. Neurosci.* 28:6714–6719. http://dx.doi.org/10.1523/JNEUROSCI.0326-08.2008

Noseda, R., S. Belin, F. Piguet, I. Vaccari, S. Scarlino, P. Brambilla, F. Martinelli Boneschi, M.L. Feltri, L. Wrabetz, A. Quattrini, et al. 2013. DDIT4/REDD1/RTP801 is a novel negative regulator of Schwann cell myelination. *J. Neurosci.* 33:15295–15305. http://dx.doi.org/10.1523/JNEUROSCI.2408-13.2013

Okuda, T., Y. Higashi, K. Kokame, C. Tanaka, H. Kondoh, and T. Miyata. 2004. Ndrg1-deficient mice exhibit a progressive demyelinating disorder of peripheral nerves. *Mol. Cell. Biol.* 24:3949–3956. http://dx.doi.org/10.1128/MCB.24.9.3949-3956.2004

Ozçelik, M., L. Cotter, C. Jacob, J.A. Pereira, J.B. Relvas, U. Suter, and N. Tricaud. 2010. Pals1 is a major regulator of the epithelial-like polarization and the extension of the myelin sheath in peripheral nerves. *J. Neurosci.* 30:4120–4131. http://dx.doi.org/10.1523/JNEUROSCI.5185-09.2010

Pearce, L.R., E.M. Sommer, K. Sakamoto, S. Wullschleger, and D.R. Alessi. 2011. Protor-1 is required for efficient mTORC2-mediated activation of SGK1 in the kidney. *Biochem. J.* 436:169–179. http://dx.doi.org/10.1042/BJ20102103

Pedraza, L., G.C. Owens, L.A. Green, and J.L. Salzer. 1990. The myelin-associated glycoproteins: membrane disposition, evidence of a novel disulfide linkage between immunoglobulin-like domains, and posttranslational palmitylation. *J. Cell Biol.* 111:2651–2661. http://dx.doi.org/10.1083/jcb.111.6.2651

Pereira, J.A., Y. Benninger, R. Baumann, A.F. Gonçalves, M. Ozçelik, T. Thurnherr, N. Tricaud, D. Meijer, R. Fässler, U. Suter, and J.B. Relvas. 2009. Integrin-linked kinase is required for radial sorting of axons and Schwann cell remyelination in the peripheral nervous system. *J. Cell Biol.* 185:147–161. http://dx.doi.org/10.1083/jcb.200809008

Pereira, J.A., F. Lebrun-Julien, and U. Suter. 2012. Molecular mechanisms regulating myelination in the peripheral nervous system. *Trends Neurosci.* 35:123–134. http://dx.doi.org/10.1016/j.tins.2011.11.006

Reiske, H.R., S.C. Kao, L.A. Cary, J.L. Guan, J.F. Lai, and H.C. Chen. 1999. Requirement of phosphatidylinositol 3-kinase in focal adhesion kinase-promoted cell migration. *J. Biol. Chem.* 274:12361–12366. http://dx.doi.org/10.1074/jbc.274.18.12361

Richie, J.M. 1984. Physiological basis of conduction in myelinated nerve fibers in myelin. P. Morell, editor. Plenum Press, New York. 117-146.

Rivard, N. 2009. Phosphatidylinositol 3-kinase: a key regulator in adherens junction formation and function. *Front Biosci (Landmark Ed)*. 14:510–522. http://dx.doi.org/10.2741/3259

Saito, F., S.A. Moore, R. Barresi, M.D. Henry, A. Messing, S.E. Ross-Barta, R.D. Cohn, R.A. Williamson, K.A. Sluka, D.L. Sherman, et al. 2003. Unique role of dystroglycan in peripheral nerve myelination, nodal structure, and sodium channel stabilization. *Neuron*. 38:747–758. http://dx.doi.org/10.1016/S0896-6273(03)00301-5

Salzer, J.L. 2012. Axonal regulation of Schwann cell ensheathment and myelination. *J. Peripher. Nerv. Syst.* **17**(s3, Suppl 3):14–19. http://dx.doi.org/10.1111/j.1529-8027.2012.00425.x

Sandoval, G.J., D.B. Graham, G.B. Gmyrek, H.M. Akilesh, K. Fujikawa, B. Sammut, D. Bhattacharya, S. Srivatsan, A. Kim, A.S. Shaw, et al. 2013. Novel Mechanism of Tumor Suppression by Polarity Gene Discs Large 1 (DLG1) Revealed in a Murine Model of Pediatric B-ALL. *Cancer Imm. Res*. 1:426–437. http://dx.doi.org/10.1158/2326-6066.CIR-13-0065

Sarbassov, D.D., D.A. Guertin, S.M. Ali, and D.M. Sabatini. 2005. Phosphorylation and regulation of Akt/PKB by the rictor-mTOR complex. *Science*. 307:1098–1101. http://dx.doi.org/10.1126/science.1106148

Sherman, D.L., and P.J. Brophy. 2005. Mechanisms of axon ensheathment and myelin growth. *Nat. Rev. Neurosci.* 6:683–690. http://dx.doi.org/10.1038/nrn1743

Sherman, D.L., M. Krols, L.M. Wu, M. Grove, K.A. Nave, Y.G. Gangloff, and P.J. Brophy. 2012. Arrest of myelination and reduced axon growth when Schwann cells lack mTOR. *J. Neurosci.* 32:1817–1825. http://dx.doi.org/10.1523/JNEUROSCI.4814-11.2012

Sommer, E.M., H. Dry, D. Cross, S. Guichard, B.R. Davies, and D.R. Alessi. 2013. Elevated SGK1 predicts resistance of breast cancer cells to Akt inhibitors. *Biochem. J.* 452:499–508. http://dx.doi.org/10.1042/BJ20130342

Spiegel, I., K. Adamsky, Y. Eshed, R. Milo, H. Sabanay, O. Sarig-Nadir, I. Horresh, S.S. Scherer, M.N. Rasband, and E. Peles. 2007. A central role for Necl4 (SynCAM4) in Schwann cell-axon interaction and myelination. *Nat. Neurosci.* 10:861–869. http://dx.doi.org/10.1038/nn1915

Spinardi, L., S. Einheber, T. Cullen, T.A. Milner, and F.G. Giancotti. 1995. A recombinant tail-less integrin beta 4 subunit disrupts hemidesmosomes, but does not suppress alpha 6 beta 4-mediated cell adhesion to laminins. *J. Cell Biol.* 129:473–487. http://dx.doi.org/10.1083/jcb.129.2.473

Taveggia, C., G. Zanazzi, A. Petrylak, H. Yano, J. Rosenbluth, S. Einheber, X. Xu, R.M. Esper, J.A. Loeb, P. Shrager, et al. 2005. Neuregulin-1 type III determines the ensheathment fate of axons. *Neuron*. 47:681–694. http://dx.doi.org/10.1016/j.neuron.2005.08.017

Terada, N., Y. Saitoh, N. Ohno, M. Komada, J. Yamauchi, and S. Ohno. 2013. Involvement of Src in the membrane skeletal complex, MPP6-4.1G, in Schmidt-Lanterman incisures of mouse myelinated nerve fibers in PNS. *Histochem. Cell. Biol*. 140:213–222. http://dx.doi.org/10.1007/s00418-012-1073-6

Thomanetz, V., N. Angliker, D. Cloëtta, R.M. Lustenberger, M. Schweighauser, F. Oliveri, N. Suzuki, and M.A. Rüegg. 2013. Ablation of the mTORC2 component rictor in brain or Purkinje cells affects size and neuron morphology. *J. Cell Biol.* 201:293–308. http://dx.doi.org/10.1083/jcb.201205030

Troussard, A.A., N.M. Mawji, C. Ong, A. Mui, R. St -Arnaud, and S. Dedhar. 2003. Conditional knock-out of integrin-linked kinase demonstrates an essential role in protein kinase B/Akt activation. *J. Biol. Chem.* 278:22374–22378. http://dx.doi.org/10.1074/jbc.M303083200

Vartanian, T., A. Goodearl, A. Viehöver, and G. Fischbach. 1997. Axonal neuregulin signals cells of the oligodendrocyte lineage through activation of HER4 and Schwann cells through HER2 and HER3. *J. Cell Biol.* 137:211–220. http://dx.doi.org/10.1083/jcb.137.1.211

Wallquist, W., S. Plantman, S. Thams, J. Thyboll, J. Kortesmaa, J. Lännergren, A. Domogatskaya, S.O. Ogren, M. Risling, H. Hammarberg, et al. 2005. Impeded interaction between Schwann cells and axons in the absence of laminin alpha4. *J. Neurosci.* 25:3692–3700. http://dx.doi.org/10.1523/JNEUROSCI.5225-04.2005

Wolpowitz, D., T.B.A. Mason, P. Dietrich, M. Mendelsohn, D.A. Talmage, and L.W. Role. 2000. Cysteine-rich domain isoforms of the *neuregulin-1* gene are required for maintenance of peripheral synapses. *Neuron*. 25:79–91. http://dx.doi.org/10.1016/S0896-6273(00)80873-9

Wulff, P., V. Vallon, D.Y. Huang, H. Völkl, F. Yu, K. Richter, M. Jansen, M. Schlünz, K. Klingel, J. Loffing, et al. 2002. Impaired renal Na(+) retention in the sgk1-knockout mouse. *J. Clin. Invest.* 110:1263–1268. http://dx.doi.org/10.1172/JCI0215696

Yu, W.M., M.L. Feltri, L. Wrabetz, S. Strickland, and Z.L. Chen. 2005. Schwann cell-specific ablation of laminin gamma1 causes apoptosis and prevents proliferation. *J. Neurosci.* 25:4463–4472. http://dx.doi.org/10.1523/JNEUROSCI.5032-04.2005

Zhang, H., X. Zha, Y. Tan, P.V. Hornbeck, A.J. Mastrangelo, D.R. Alessi, R.D. Polakiewicz, and M.J. Comb. 2002. Phosphoprotein analysis using antibodies broadly reactive against phosphorylated motifs. *J. Biol. Chem.* 277:39379–39387. http://dx.doi.org/10.1074/jbc.M206399200